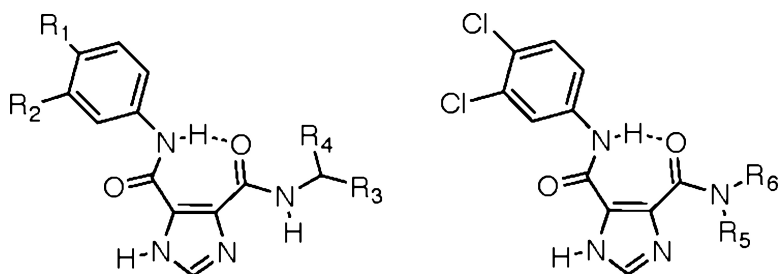


Imidazole-4,5-dicarboxamide Derivatives with Antiproliferative Activity against HL-60 Cells

Elisabeth M. Perchellet, Jean-Pierre Perchellet, and Paul W. Baures

J. Med. Chem., **2005**, 48 (19), 5955-5965 • DOI: 10.1021/jm050160r • Publication Date (Web): 23 August 2005

Downloaded from <http://pubs.acs.org> on March 28, 2009



More About This Article

Additional resources and features associated with this article are available within the HTML version:

- Supporting Information
- Access to high resolution figures
- Links to articles and content related to this article
- Copyright permission to reproduce figures and/or text from this article

[View the Full Text HTML](#)

Imidazole-4,5-dicarboxamide Derivatives with Antiproliferative Activity against HL-60 Cells

Elisabeth M. Perchellet,[†] Jean-Pierre Perchellet,[†] and Paul W. Baures^{*‡}

Anti-Cancer Drug Laboratory, Kansas State University, Division of Biology, Ackert Hall, Manhattan, Kansas 66506-4901, and Department of Chemistry, Bowdoin College, 6600 College Station, Brunswick, Maine 04011

Received February 18, 2005

A series of *N,N'*-disubstituted imidazole-4,5-dicarboxamides (I45DCs) were prepared and tested in order to determine their antiproliferative activity against HL-60 cells. The design of the I45DCs was based in part on the structures of trisubstituted purines complexed with cyclin dependent kinase 2 (cdk2), a protein important in regulating the G1/S transition in the cell cycle, and the intramolecular hydrogen bond in I45DCs that predisposes the conformation to one that mimics substituted adenosines. A majority of the I45DCs in this study inhibit proliferation of HL-60 cells as measured by an MTS mitochondrial functional assay with IC₅₀'s in the 2.5–25 μM range. The SAR of the I45DCs is consistent with anticipated hydrogen bonding interactions in the ATP-binding site of cdk2. Thus, the I45DCs represent a useful scaffold for anticancer lead discovery that is both readily accessible and easily diversified.

Introduction

Cancer cells share certain characteristics irrespective of their origin, the tissue involved, or the stage of growth, including the ability to grow unchecked.¹ A cancer cell acquires such immortality through mechanisms that sidetrack those biochemical pathways that normally check cellular viability and control growth.² For example, the cell cycle operates through a series of checks and balances that determine whether a cell can proceed to the next stage or whether the cell is damaged and should instead abort division.³ One such checkpoint in the cell cycle transition between the initial growth phase (G₁) and the synthesis phase (S) requires the interplay of cyclins and cyclin-dependent kinases (cdk), including an association between cyclin E and cdk2.^{4–6}

Kinases form one of the largest protein families in the human genome and have an important role in signal transduction within the cell.^{7,8} As noted above, kinases are at the center of events that control the cell cycle and as such are valued targets for cancer.^{9–13} There remains an open question about whether specific or nonspecific kinase inhibitors will ultimately prove to be the more valuable in treating cancer.⁹ Thus, there is a need for new kinase inhibitor classes to help guide optimal selection of clinical candidates.¹⁴ This is particularly relevant as questions have arisen regarding the ability of cells to either bypass or substitute for the role of cdk2 in the cell cycle.^{15–17} On the other hand, flavopiridol was discovered as a cdk2 inhibitor and is showing value in the clinical treatment of cancer,¹⁸ although this may be through a combination of effects.¹⁹

Many compound classes interfere with kinase activity by binding competitively to the ATP binding site.^{11,20–22} X-ray crystallography of kinase complexes with inhibi-

tors across structural classes finds that hydrogen bonding between the inhibitor and backbone N–H and C=O functionalities is a common feature between the inhibitor classes.¹¹ These hydrogen bonds have been prominently featured in structure-based drug design projects against kinase targets.^{23,24} A portion of the hydrogen bonding interactions to ATP,²⁵ olomoucine,²⁶ purvalanol B,²⁷ and flavopiridol²⁸ in the cdk2 binding site are illustrated in Figure 1.

This paper describes derivatives of the imidazole-4,5-dicarboxylic acid (I45DA) scaffold that exhibit antiproliferative activity against HL-60 cells. We reasoned that inhibition of kinases important to the cell cycle could be inferred through cell antiproliferative activity measurements, much as recently reported for MCS–C2.²⁹ The *N,N'*-disubstituted imidazole-4,5-dicarboxamides (I45DCs) in this study are capable of forming intermolecular pairwise hydrogen bonds that could serve as an “anchor” within an ATP binding site of a kinase, in a similar manner as established for olomoucine and purvalanol, and knew that pairwise hydrogen bonds were significant interactions in the observed solid-state packing arrangements of similar I45DCs.³⁰ We chose substituents for our starting I45DCs on the basis of olomoucine and purvalanol B, as well as known structural SAR patterns from the literature.^{31,32} Modifications to the starting set of I45DCs were designed in order to probe the binding site for favorable interactions, identify sterically accessible sites, and determine whether the HL-60 antiproliferative activity data for the I45DCs paralleled expectations of cdk2 binding.

Results and Discussion

Chemistry. The I45DCs in this study were prepared from **1**, a compound that contains both reactive acid chloride and acyl imidazole functionality. This compound is prepared from imidazole-4,5-dicarboxylic acid by a method previously reported.³³ The synthesis of *N,N'*-dissymmetrically disubstituted I45DCs with only primary alkanamines requires the formation of a phenyl

* To whom correspondence should be addressed. Current address: Department of Chemistry, University of Tulsa, Tulsa, OK 74104. Phone: 918-631-3024. E-mail: paul-baures@utulsa.edu.

[†] Kansas State University.

[‡] Bowdoin College.

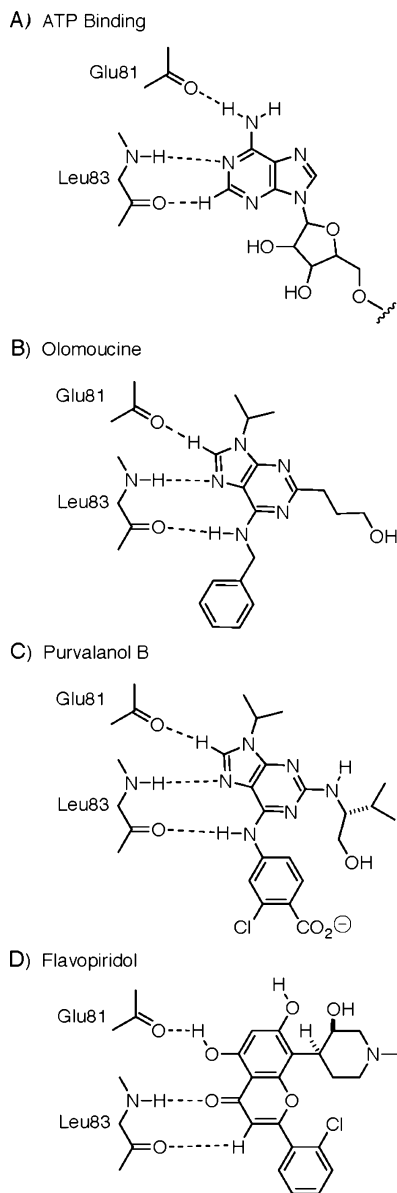
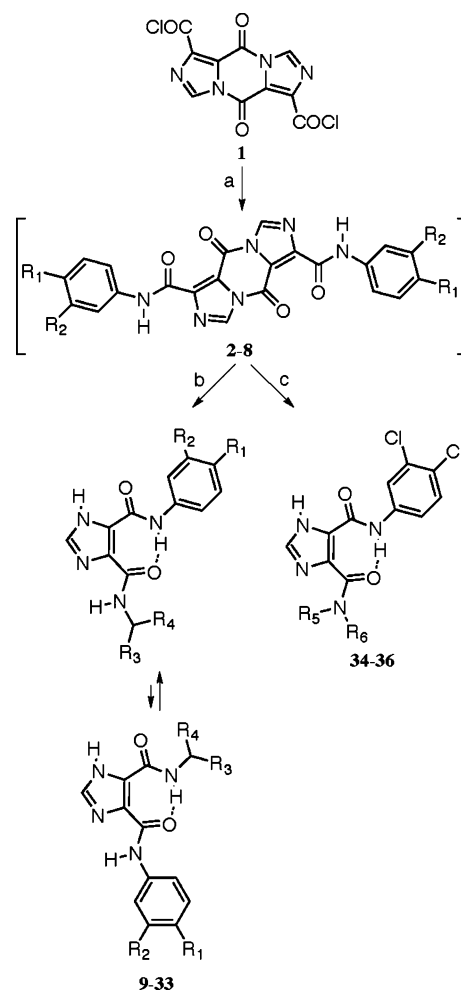


Figure 1. Comparison of hydrogen bonding interactions between protein kinase backbone amides (labeling is shown according to cdk2 structures) with (A) ATP (B) olomoucine, (C) purvalanol B, and (D) flavopiridol. In all examples the protein kinase and inhibitor associate through a combination of strong (OH \cdots O, NH \cdots O, and NH \cdots N) and relatively weak hydrogen bonds (CH \cdots O).

ester intermediate in order to effectively differentiate the two different reactive functionalities of **1**.³³ On the other hand, amino acid esters afford enough selectivity between the acid chloride and acyl imidazole reactivity in order to be useful for the synthesis of *N,N'*-disubstituted I45DCs bearing amino acid esters.³⁴ In similar fashion, anilines react selectively to yield **2–8**, intermediates that were then reacted with alkanamines or amino acid esters to yield the product I45DCs, **9–36**, used for this study (Scheme 1).

Pyrazines **2–8** were obtained from the addition of the appropriate aniline (2 equiv) and *N,N*-diethylaniline (2 equiv) that serves as a scavenger for the acid produced in the reaction. These are heterogeneous reactions and the product solids are isolated by vacuum filtration before partial purification through a series of washings. The pyrazines were then used to synthesize the desired

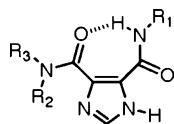
Scheme 1^a



I45DCs by addition of an alkanamine or free amino acid ester. The final products were purified by silica gel chromatography before characterization by ¹H and ¹³C NMR spectroscopy, mass spectrometry, and RP-HPLC.

Antiproliferative Activity Measurements. Compounds **9–36** were tested for their antiproliferative activity against HL-60 cells at 2 and 4 days (Table 1). Briefly, the I45DCs were dissolved in DMSO, serially diluted, and added to HL-60 cells in 1 μ L aliquots. The cells were incubated for 2 or 4 days before determining their mitochondrial ability to bioreduce the tetrazolium dye MTS to a formazan product that absorbs at 490 nm.³⁵ The absorbance was corrected for blank values from culture medium alone, and the results analyzed as previously reported.³⁶

In selecting the starting I45DC, we chose a 3,4-dichloroaniline substituent rather than the 3-chloro-4-carboxyaniline present in purvalanol B. This substitution seemed reasonable since the absence of the carboxy group yields purvalanol A, a compound that is also a kinase inhibitor.^{27,37} In addition, purvalanol B is inactive on cells, possibly due to an inability to cross cell membranes with the presence of a charged functional group.³⁸ The second I45DC substituent was then varied in order to obtain a structure–activity relationship at the R₃ position of this scaffold. The initial compound, **9**, bears an alkylamine as a partial mimic of the second

Table 1. Antiproliferative Activity of *N,N'*-Dissymmetrically Disubstituted I45DCs in HL-60 Cells

compound	R ₁	R ₂	R ₃	HL-60 cells: IC ₅₀ (μM)	
				day 2 ^a	day 4 ^a
9	3,4-Cl ₂ C ₆ H ₃	H	CH ₂ CH(CH ₃) ₂	14.7 ± 0.9	7.2 ± 0.8
10	3,4-Cl ₂ C ₆ H ₃	H	cyclo(C ₆ H ₁₁)	33.1 ± 1.9	12.3 ± 1.1
11	3,4-Cl ₂ C ₆ H ₃	H	(CH ₂) ₅ CH ₃	14.6 ± 1.0	7.8 ± 0.5
12	3,4-Cl ₂ C ₆ H ₃	H	CH ₂ Ph	11.5 ± 0.5	7.4 ± 0.4
13	3,4-Cl ₂ C ₆ H ₃	H	CH ₂ CH ₂ Ph	17.7 ± 1.3	13.2 ± 0.8
14	3,4-Cl ₂ C ₆ H ₃	H	CH ₂ -4-Cl-Ph	16.2 ± 1.5	8.8 ± 0.3
15	3,4-Cl ₂ C ₆ H ₃	H	CH ₂ -4-CH ₃ -Ph	21.4 ± 0.9	15.2 ± 0.4
16	3,4-Cl ₂ C ₆ H ₃	H	CH ₂ -4-OCH ₃ -Ph	24.3 ± 1.0	18.3 ± 1.6
17	3,4-Cl ₂ C ₆ H ₃	H	CH ₂ -4-Ph-Ph	7.0 ± 0.4	2.9 ± 0.3
18	3,4-Cl ₂ C ₆ H ₃	H	(<i>R</i>)-CHCH ₃ Ph	8.8 ± 0.3	5.9 ± 0.6
19	3,4-Cl ₂ C ₆ H ₃	H	(<i>S</i>)-CHCH ₃ Ph	9.2 ± 0.4	5.9 ± 0.6
20	3,4-Cl ₂ C ₆ H ₃	H	CH ₂ CO ₂ C(CH ₃) ₃	49.8 ± 5.2	25.4 ± 2.8
21	3,4-Cl ₂ C ₆ H ₃	H	(<i>R</i>)-CHCH ₃ CO ₂ CH ₃	> 62.5	> 62.5
22	3,4-Cl ₂ C ₆ H ₃	H	(<i>R</i>)-CHCH ₃ CO ₂ C(CH ₃) ₃	4.6 ± 0.5	2.5 ± 0.2
23	3,4-Cl ₂ C ₆ H ₃	H	(<i>S</i>)-CHCH ₃ CO ₂ C(CH ₃) ₃	4.9 ± 0.3 ^b	2.4 ± 0.1 ^b
24	3,4-Cl ₂ C ₆ H ₃	H	(<i>R</i>)-CHPhCO ₂ CH ₃	17.3 ± 1.4	10.8 ± 0.7
25	3,4-Cl ₂ C ₆ H ₃	H	(<i>S</i>)-CHPhCO ₂ CH ₃	13.2 ± 0.7	6.8 ± 0.7
26	3,4-Cl ₂ C ₆ H ₃	H	(<i>R</i>)-CH(CH(CH ₃) ₂)CO ₂ CH ₃	8.5 ± 0.7 ^c	4.9 ± 0.3 ^d
27	3,4-Cl ₂ C ₆ H ₃	H	(<i>S</i>)-CH(CH(CH ₃) ₂)CO ₂ CH ₃	> 62.5	> 62.5
28	3-ClC ₆ H ₄	H	(<i>R</i>)-CHCH ₃ CO ₂ C(CH ₃) ₃	8.2 ± 0.7 ^e	2.9 ± 0.3 ^b
29	4-ClC ₆ H ₄	H	(<i>R</i>)-CHCH ₃ CO ₂ C(CH ₃) ₃	6.6 ± 0.5 ^f	3.3 ± 0.3 ^g
30	4-CH ₃ C ₆ H ₄	H	(<i>R</i>)-CHCH ₃ CO ₂ C(CH ₃) ₃	6.3 ± 0.4 ^f	3.5 ± 0.3 ^f
31	4-OCH ₃ C ₆ H ₄	H	(<i>R</i>)-CHCH ₃ CO ₂ C(CH ₃) ₃	6.0 ± 0.5 ^g	3.1 ± 0.3 ^h
32	4-CO ₂ CH ₂ CH ₃ -C ₆ H ₄	H	(<i>R</i>)-CHCH ₃ CO ₂ C(CH ₃) ₃	6.3 ± 0.5 ^g	3.7 ± 0.4 ^f
33	C ₆ H ₅	H	(<i>R</i>)-CHCH ₃ CO ₂ C(CH ₃) ₃	4.7 ± 0.4 ^b	2.7 ± 0.1 ^b
34	3,4-Cl ₂ C ₆ H ₃	CH ₂ CH ₂ CH ₃	CH ₂ CH ₂ CH ₃	378.6 ± 25.1	38.9 ± 3.4
35	3,4-Cl ₂ C ₆ H ₃	CH ₃	(<i>R</i>)-CHCH ₃ Ph	75.5 ± 3.2	56.0 ± 3.4
36	3,4-Cl ₂ C ₆ H ₃	CH ₃	(<i>S</i>)-CHCH ₃ Ph	89.4 ± 3.0	68.8 ± 2.1

^a Concentrations of I45DCs required to inhibit by 50% the metabolic activity of human HL-60 cells at days 2 and 4 days in vitro. Cell proliferation results (means ± SD, *n* = 3) were expressed as % of the net absorbance of MTS/formazan after bioreduction by vehicle-treated control cells after 2 ($A_{490 \text{ nm}} = 1.192 \pm 0.051$, 100 ± 4.3%) and 4 days ($A_{490 \text{ nm}} = 1.235 \pm 0.057$, 100 ± 4.6%) in culture. The blank values ($A_{490 \text{ nm}} = 0.368$ at day 2 and 0.382 at day 4) for cell-free culture medium supplemented with MTS:PMS reagent were subtracted from the results. IC₅₀ values were calculated from linear regression of the slopes of the log-transformed concentration–survival curves. ^b Not different from the respective effects of **22** at days 2 and 4. ^c *P* < 0.005, ^d *P* < 0.0005, ^e *P* < 0.01, ^f *P* < 0.025, and ^g *P* < 0.05 greater than the effects of **22** at days 2 and 4. ^h *P* < 0.01, smaller than the effects of **12** at day 2.

substituent in purvalanol B, but without an added stereocenter. This compound was less active (IC₅₀ = 7.2 ± 0.8 μM) on HL-60 cells than the average growth inhibitory activity found for purvalanol A (2 μM) over the NCI 60 tumor cell lines,²¹ although it was active enough to generate optimism about improving the bioactivity through modification.

A cyclic and linear alkanamine were tested in **10** and **11**, respectively, with both compounds showing antiproliferative activity against HL-60 cells, but with **10** seemingly less active than either **9** or **11**. A benzylamine analogue, **12**, is equipotent to **9** and **11**, although a longer chain (**13**) and most 4-substituted benzylamines (**14**–**16**) yielded analogues of either weaker or comparable activity. There is an exception found in **17**, which is substituted with 4-phenylbenzylamine. Although this compound represented an improvement in biological activity (IC₅₀ = 2.9 ± 0.3 μM) over **9**–**16**, this substitution significantly increases the overall size and hydrophobicity of the molecule, and we chose to continue exploring changes to the overall substituent.

The introduction of a chiral α-methylbenzylamine generates a stereocenter in **18** and **19**, compounds with identical antiproliferative activity that is also comparable to **12**. Purvalanol B contains an analogous stereocenter and was part of the incentive for the synthesis

of these analogues. Purvalanol A is very similar to purvalanol B, but simply excludes the carboxyl substituent off the aromatic ring of purvalanol B. It is interesting that the two stereoisomers of purvalanol A inhibit the malarial parasite, *P. falciparum*, with nearly identical bioactivities, but have a 15-fold difference in bioactivity on an isolated CDK1/cyclin B complex.³⁹ The same antiproliferative activities of **18** and **19** can be attributed to the lack of a distinguishing interaction between the stereocenter and the target protein. However, it is also possible that multiple targets or other distinctions for the two enantiomers simply yield coincidental inhibition of HL-60 cell proliferation. It is not possible to distinguish between these possibilities from the available data.

The structure–activity development of the I45DC was continued with a series of amino acid esters, **20**–**27**, having similarities to the D-valinol substituent in the purvalanols. Of these, the I45DCs with the two stereoisomers of alanine *tert*-butyl ester, **22** and **23**, are the most cytostatic at 4 days (IC₅₀ ≈ 2.5 μM). Glycine *tert*-butyl ester is 10× less active at 4 days (IC₅₀ = 25.4 ± 2.8 μM). Both stereoisomers of phenylglycine methyl ester are less cytostatic (*R*: IC₅₀ = 10.8 ± 0.7 μM; *S*: IC₅₀ = 6.8 ± 0.7 μM), as is the *R*-isomer of valine methyl ester (IC₅₀ = 4.9 ± 0.3 μM). The *R*-isomer of alanine

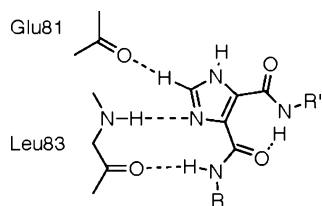


Figure 2. Potential binding mode of **22** with the cdk2 binding site.

methyl ester was inactive at 62.5 μM , as was the *S*-isomer of valine methyl ester. We hypothesize that this reflects hydrolysis of the methyl esters by action of esterases or peptidases in the HL-60 cells. Although more likely to recognize the *S*-amino acids as substrates, the small side chain of the *R*-alanine may be tolerated in a peptidase active site. Likewise, the nonnatural phenylglycine side chain in **27** could reasonably preclude productive binding. The sterically hindered *tert*-butyl esters in **20** or **23** would be poor substrates regardless of the amino acid side chain or stereochemistry.

We next made modifications to the 3,4-dichloroaniline while retaining the *R*-alanine *tert*-butyl ester, yielding **29–33**. All of these aniline variations have approximately equal antiproliferative activity on HL-60 cells (IC_{50} 's = 2.7–3.5 μM) at 4 days. This suggests steric and electronic tolerance within the binding site(s) in order to accommodate varying substituents on the aniline of the I45DCs used in this study, although it is also possible that the aniline is all or partly solvent exposed when bound. A detailed SAR around the aniline could produce selectivity against purified targets or enhanced potency on whole cells or both.

Many of the I45DCs **9–33** have two intramolecularly hydrogen bonded conformations evident in their ^1H NMR spectra taken in either CDCl_3 or $\text{DMSO-}d_6$. The ratio of conformers, when observable, is generally 7:3 or 8:2, and favors the aniline as the hydrogen bond donor (Scheme 1). This ratio was assigned from the relative integrations of the sharp singlet aniline NH (hydrogen bonded or non-hydrogen bonded), the broad imidazole NH, and the split amide NH (either doublets or triplets depending upon the substitution). The NMR data is consistent with Spartan⁴⁰ calculations using the PM3 force field that finds a $-1.07 \text{ kcal mol}^{-1}$ energy difference favoring this conformer. The intramolecular hydrogen bond for a representative I45DC has recently been determined to be worth $14 \pm 1 \text{ kcal mol}^{-1}$ at 3 mM in $\text{DMSO-}d_6$.⁴¹ This intramolecular hydrogen bond was integral to our hypothesis for bioactivity in this series and yields an overall I45DC structure for **22** that, in the less favorable conformer, is comparable to purvalanol A. With this information, it is possible to hypothesize about potential bound conformation(s) of **22**, and to use this information in subsequent designs. Our expected interactions with a target ATP binding site, such as found in cdk2, is shown in Figure 2. Three other potential binding modes were discounted on the basis of steric interference from substituents, and one formed hydrogen bonding combinations to the protein target that would be inconsistent with the aniline as the intramolecular hydrogen bond donor (see Supporting Information). The SAR data for **9–33** is consistent with Figure 2, where the aniline is the intramolecular hydrogen bond donor. The intermolecular hydrogen

bonding interactions between inhibitor and protein help favor and direct binding. This includes hydrogen bonds from CH groups, as recently shown in the inhibition of glycogen synthase kinase 3.⁴²

The similar cytotoxicities of **22**, **23**, and **29–33** are likely a sign of steric and electronic tolerance within the binding site(s). We reason that the aniline can either accept a hydrogen bonding interaction from a Lys $\epsilon\text{-NH}_3^+$ to its substituent(s) or form $\text{NH}\cdots\pi$ interactions with the ring. On the other hand, the cytotoxicities of **34–36** are 5–11 times less active than comparable I45DCs in this study (*i.e.*, **34** versus **9**, **35** versus **18**, and **36** versus **19**). These provide additional evidence in support of this potential target and binding interaction, as the antiproliferative activity differences between **35** and **18**, for example, is explained in terms of the *N*-methyl group blocking pairwise hydrogen bonding of the I45DC with Leu83 in cdk2 (Figure 2). The observed log unit difference in activity can be attributed to the loss of a hydrogen bond to the Leu83 carbonyl oxygen, potentially leaving **34–36** to form a single hydrogen bond to the protein target, analogous to that observed for the pyridinylimidazole class of P38 MAP kinase inhibitors.²⁰ Alkylation of the imidazole ring in **22** would also favor a single I45DC conformation, and in this case the intramolecular hydrogen bond donor is on the same side as the alkylated nitrogen.⁴¹ Thus, short alkyl chains on the same side of the imidazole ring as the aniline substituent could provide more potent compounds, as these chains compare with the isopropyl group in purvalanol A/B. These substitutions will be part of future investigations in the I45DC class.

Comparative Antiproliferative Activity Measurements. Based on their increasing ability to inhibit HL-60 cell proliferation at 2 and 4 days, the antitumor activity of I45DC derivatives is a combination of drug concentration and duration of action (Table 1 and Figure 3). In contrast to olomoucine (IC_{50} : 108.6 μM at day 2 and 77.9 μM at day 4), which is the least effective of the reference cdk2 inhibitors tested against HL-60 cell proliferation, **22** (IC_{50} : 4.6 μM at day 2 and 2.5 μM at day 4) is an interesting cytostatic agent at least as good as, or even slightly better than, purvalanol A (IC_{50} : 11.3 μM at day 2 and 4.8 μM at day 4), although it does not match the superior antiproliferative activity of flavopiridol (IC_{50} : 129 nM at day 2 and 82 nM at day 4) in this tumor cell system (Figure 3). Overall, the antiproliferative activity of **22** is about 30.5–35.6 times lower than that of flavopiridol but 1.9–2.5 and 23.6–31.2 times higher than those of purvalanol A and olomoucine, respectively (Figure 3). The 842–950-fold difference between the antiproliferative activities of olomoucine and flavopiridol observed in our HL-60 study is in agreement with the report that flavopiridol shows cytostatic and cytotoxic effects at the same concentration that is required *in vitro* for cdk inhibition (10^{-7} range), whereas 10–100 times higher concentrations of olomoucine are required for cell growth suppression than those needed to inhibit cdk activity *in vitro*.⁴³

Inhibition of DNA Synthesis. In HL-60 cells incubated for 2.5 h with **22**, the concentration-dependent inhibition of DNA synthesis starts at 1.6 μM and is maximal at 25 μM (Figure 4A). Compound **22** (IC_{50} : 4.13 μM) inhibits DNA synthesis to a lesser degree than

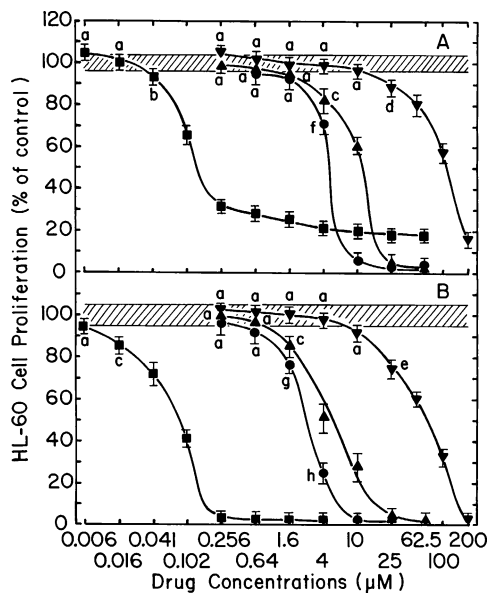


Figure 3. Comparison of the abilities of serial concentrations (plotted on a logarithmic scale) of **22** (●), flavopiridol (■), purvalanol A (▲) and olomoucine (▼) to inhibit the metabolic activity of HL-60 cells at days 2 (A) and 4 (B) in vitro. Cell proliferation results were expressed as % of the net absorbance of MTS/formazan after bioreduction by vehicle-treated control cells after 2 ($A_{490\text{ nm}} = 1.429 \pm 0.055$, $100 \pm 3.8\%$, striped area in A) and 4 ($A_{490\text{ nm}} = 1.332 \pm 0.067$, $100 \pm 5.1\%$, striped area in B) days in culture. The blank values ($A_{490\text{ nm}} = 0.347$ at day 2 and 0.346 at day 4) for cell-free culture medium supplemented with MTS/PMS reagent were subtracted from the results. Bars: means \pm SD ($n = 3$). ^aNot different from respective controls; ^b $P < 0.05$, ^c $P < 0.025$, ^d $P < 0.01$ and ^e $P < 0.005$, smaller than respective controls; ^f $P < 0.005$, smaller than control and $P < 0.05$, smaller than $4\ \mu\text{M}$ purvalanol A; ^g $P < 0.005$, smaller than control and $P < 0.025$, smaller than $1.6\ \mu\text{M}$ purvalanol A; ^h $P < 0.005$, smaller than $4\ \mu\text{M}$ purvalanol A.

flavopiridol (IC_{50} : $0.96\ \mu\text{M}$) but is almost as effective as purvalanol A (IC_{50} : $2.14\ \mu\text{M}$) and much more potent than olomoucine (IC_{50} : $46.8\ \mu\text{M}$). As inhibitor of DNA synthesis, therefore, **22** is 11.3 times more potent than olomoucine and only 1.9 and 4.3 times less effective than purvalanol A and flavopiridol, respectively (Figure 4A). Although it may be somewhat misleading to compare IC_{50} values for responses measured at very different times, the abilities of **22**, purvalanol A, flavopiridol, and olomoucine to inhibit DNA synthesis at 2.5 h (Figure 4A) generally match their antiproliferative activities in the HL-60 cell system at 2–4 days (Figure 3), suggesting that their effectiveness as inhibitors of DNA synthesis may play a major role in their mechanism of antitumor activity. Interestingly, at concentrations greater than $4\ \mu\text{M}$, **22** and purvalanol A both appear to inhibit DNA synthesis at 2.5 h (Figure 4A) and HL-60 cell proliferation at day 2 (Figure 3A) to a greater degree than flavopiridol. Since this effect disappears at day 4 (Figure 3B), high concentrations of **22** and purvalanol A may reach their maximal inhibitory potential more rapidly than those of flavopiridol. In addition, because tumor cells undergoing replicative senescence are as sensitive to flavopiridol as rapidly dividing metastasized cancer cells, the mechanism of flavopiridol action may not be dependent on the activity of cyclin-dependent kinases that regulate cell cycle progression.⁴⁴

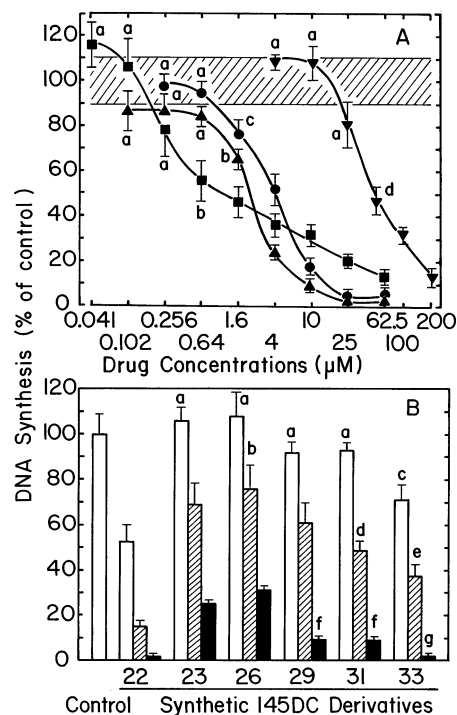


Figure 4. I45DC derivatives inhibit DNA synthesis in HL-60 cells. A, Comparison of the abilities of serial concentrations (plotted on a logarithmic scale) of **22** (●), flavopiridol (■), purvalanol A (▲) and olomoucine (▼) to inhibit the rate of incorporation of [³H]-thymidine into DNA measured in HL-60 cells over 30 min following a 2 h period of incubation at $37\ ^\circ\text{C}$ in vitro. DNA synthesis in vehicle-treated control cells at $37\ ^\circ\text{C}$ was $14,399 \pm 1,526\ \text{cpm}$ ($100 \pm 10.6\%$, striped area). The blank value ($721 \pm 67\ \text{cpm}$) for control cells incubated and pulse-labeled at $2\ ^\circ\text{C}$ with $1\ \mu\text{C}$ of [³H]-thymidine has been subtracted from the results. Bars: means \pm SD ($n = 3$). ^aNot different from control; ^b $P < 0.01$, ^c $P < 0.05$ and ^d $P < 0.005$, smaller than control. B, Comparison of the abilities of 4 (open columns), 10 (striped columns) and $25\ \mu\text{M}$ (closed columns) concentrations of selected I45DCs to inhibit DNA synthesis in HL-60 cells at 2.5 h. After subtracting the blank ($858 \pm 84\ \text{cpm}$), the value of the untreated control is $12,427 \pm 1,056\ \text{cpm}$ ($100 \pm 8.5\%$, striped area). ^aNot different from control; ^b $P < 0.05$, smaller than control; ^c $P < 0.01$, smaller than control and $P < 0.05$, greater than $4\ \mu\text{M}$ **22**; ^d $P < 0.05$, smaller than $10\ \mu\text{M}$ **23**; ^e $P < 0.05$, smaller than $10\ \mu\text{M}$ **31** and $P < 0.005$, greater than $10\ \mu\text{M}$ **22**; ^f $P < 0.0005$, smaller than $25\ \mu\text{M}$ **23**; ^gNot different from $25\ \mu\text{M}$ **22** but $P < 0.005$, smaller than $25\ \mu\text{M}$ **31**.

The effectiveness of selected I45DC derivatives against DNA synthesis in HL-60 cells (Figure 4B) was compared to that of **22**, since the antitumor effects of this lead compound (Table 1) on DNA synthesis (Figure 4A) and tumor cell proliferation (Figure 3) nearly match those of the reference cdk2 inhibitor purvalanol A. With some exception, all I45DC derivatives decrease in a concentration-dependent manner the rate of incorporation of ³H-thymidine into DNA at 2.5 h in relation with their antiproliferative activity at 2–4 days, substantiating the link between these two inhibitory events. On an equimolar concentration basis, **22** is clearly the most potent and **33** nearly matches its effect, whereas **26** is the least effective of the selected I45DCs tested against DNA synthesis (Figure 4B). It should be noted that **22** and **33** are the only compounds that significantly reduce DNA synthesis at $4\ \mu\text{M}$ and totally abolish this process at $25\ \mu\text{M}$. The other I45DCs share intermediate poten-

cies, although compounds **29** and **31** inhibit DNA synthesis more effectively than compound **23** at 25 μM .

Taken together, these results suggest that synthetic I45DCs, such as **22** and **33**, which can inhibit DNA synthesis (Figure 4) and tumor cell proliferation (Table 1 and Figure 3) in the same μM range as purvalanol A, might be valuable to develop new means of polychemotherapy.

Conclusion

The I45DCs tested in this study are cytostatic to HL-60 cells at 2 and 4 days, with potencies for the most active being comparable to those described for initial lead compounds in other classes under investigation.^{27,29,37,38,45} The observed antiproliferative activities of the I45DCs do not confirm a specific mechanism of action or target protein. Nonetheless, the SAR of the I45DCs hydrogen bonding features is consistent with our hypothesis that these interactions may direct the I45DC binding to an ATP site of either cdk2 or similar kinases.

The I45DCs are an easily accessible and useful structural class for anticancer drug discovery. It is expected that the I45DCs can be optimized with respect to either antiproliferative activity against a given tumor cell line or for inhibition against an isolated protein target such as a kinase.

Experimental Section

Synthesis and Purification of I45DCs. General Methods. All apparatus were oven-dried and cooled in a desiccator. Reagent grade solvents and other reagents were purchased from commercial suppliers and used without purification. Thin-layer chromatography was done on 250 μm silica gel plates containing a fluorescent indicator and were visualized by using UV and I_2 as well as ninhydrin spray for amines. Melting points are uncorrected. ^1H and ^{13}C NMR spectra were measured at 400 and 100.6 MHz, respectively, in either CDCl_3 with CHCl_3 as the internal reference for ^1H (δ 7.26) and CDCl_3 as the internal reference for ^{13}C (δ 77.06) or in $\text{DMSO}-d_6$ with DMSO as the internal reference for ^1H (δ 2.50) and $\text{DMSO}-d_6$ as the internal reference for ^{13}C (δ 39.50). Mass spectroscopy was done on a HiResMALDI Fourier transform mass spectrometer (IonSpec, Irvine, CA) with a Cryomagnetics (Oak Ridge, TN) 4.7 T actively shielded superconducting magnet. Ions were generated by MALDI with a pulsed nitrogen laser at 337 nm and the spectra were calibrated from 2,5-dihydroxybenzoic acid matrix peaks.

Homogeneity of **9–36** was determined by RP-C18 HPLC analysis. Samples were prepared at a concentration of 1 mg/mL in methanol, except for **10** and **14–17**, which were less soluble and therefore diluted from their $\text{DMSO}-d_6$ NMR solutions into methanol in order to yield approximately 1 mg/mL samples ($\leq 10\%$ $\text{DMSO}-d_6$). Five or fifteen microliters of the sample was eluted on a C18-RP analytical column with one of two different gradients of acetonitrile/water at a 1 mL/min flow rate. Compounds were detected at 218 nm. The two gradients used were as follows: method A, 0 min., 1:1 $\text{CH}_3\text{CN}/\text{H}_2\text{O} \rightarrow 10$ min., 19:1 $\text{CH}_3\text{CN}/\text{H}_2\text{O} \rightarrow 12$ min., $\text{CH}_3\text{CN} \rightarrow 14$ min.; method B, 0 min., 1:1 $\text{CH}_3\text{CN}/\text{H}_2\text{O} \rightarrow 10$ min., 19:1 $\text{CH}_3\text{CN}/\text{H}_2\text{O} \rightarrow 12$ min., $\text{CH}_3\text{CN} \rightarrow 29$ min., $\text{CH}_3\text{CN} \rightarrow 30$ min., 1:1 $\text{CH}_3\text{CN}/\text{H}_2\text{O}$.

Aniline-Substituted Pyrazines (2–8). General Procedure. To a round-bottom flask was suspended **1** in either ethyl acetate or dichloromethane. To this stirred suspension was added all at once *N,N*-diethylaniline (2.0–2.2 equiv.) followed by the primary aniline (2.0–2.6 equiv.). The reaction mixture was stirred at room temperature for 2–16 h before collecting the colored solid by vacuum filtration. The product was washed with portions of solvent, cold water, and acetone, respectively.

The resulting solid was allowed to air-dry and was used without further purification. In some cases the product retains trace *N,N*-diethylaniline through the wash steps.

***N,N'*-Di-3,4-dichlorophenyl-5,10-dioxo-5*H*,10*H*-diimidazo[1,5-*a*:1'-5'-*d*]pyrazine-1,6-dicarboxamide (2).** Synthesized from 0.750 g of **1** (2.40 mmol), 0.81 mL of *N,N*-diethylaniline (5.03 mmol), and 1.00 g of 3,4-dichloroaniline (6.17 mmol) in 10 mL of ethyl acetate, stirring 16 h to yield 1.19 g of crude **2** (88% yield) as a tan solid: mp 257–258 °C (dec); ^1H NMR ($\text{DMSO}-d_6$) δ 11.01 (s, 2 H), 9.11, 9.10 (s, 2 H), 8.10–8.30 (m, 2 H), 7.64–7.80 (m, 4 H); ^{13}C NMR ($\text{DMSO}-d_6$) δ 159.2, 158.2, 148.5, 143.9, 138.3, 135.3, 131.0, 130.6, 128.6, 125.7, 121.1, 120.9, 120.0.

***N,N'*-Di-3-chlorophenyl-5,10-dioxo-5*H*,10*H*-diimidazo[1,5-*a*:1'-5'-*d*]pyrazine-1,6-dicarboxamide (3).** Synthesized from 0.163 g of **1** (0.521 mmol), 167 μL of *N,N*-diethylaniline (1.04 mmol), and 110 μL of 3-chloroaniline (1.04 mmol) in 3 mL of ethyl acetate, stirring 2 h to yield 0.218 g of crude **3** (85% yield) as a light yellow solid: mp 250–252 °C (dec); ^1H NMR ($\text{DMSO}-d_6$) δ 10.89 (s, 2 H), 9.11 (s, 2 H), 7.99, 7.93 (m, 2 H), 7.64–7.72 (m, 2 H), 7.41–7.45 (m, 2 H), 7.21–7.26 (m, 2 H); ^{13}C NMR ($\text{DMSO}-d_6$) δ 160.2, 159.1, 145.3, 140.6, 139.4, 138.6, 136.4, 133.9, 131.4, 129.6, 125.6, 124.9, 121.7, 120.3, 119.4.

***N,N'*-Di-4-chlorophenyl-5,10-dioxo-5*H*,10*H*-diimidazo[1,5-*a*:1'-5'-*d*]pyrazine-1,6-dicarboxamide (4).** Synthesized from 0.168 g of **1** (0.537 mmol), 172 μL of *N,N*-diethylaniline (1.07 mmol), and 0.137 g of 4-chloroaniline (1.07 mmol) in 3 mL of ethyl acetate, stirring 2 h to yield 0.227 g of crude **4** (85% yield) as a red solid: mp 250–252 °C (dec); ^1H NMR ($\text{DMSO}-d_6$) δ 10.85 (s, 2 H), 9.09 (s, 2 H), 7.79–7.85 (m, 4 H), 7.45–7.47 (m, 4 H); ^{13}C NMR ($\text{DMSO}-d_6$) δ 159.1, 157.9, 148.6, 144.4, 138.3, 137.0, 135.9, 135.3, 128.6, 128.5, 127.8, 122.7, 121.4, 120.4.

***N,N'*-Di-4-methylphenyl-5,10-dioxo-5*H*,10*H*-diimidazo[1,5-*a*:1'-5'-*d*]pyrazine-1,6-dicarboxamide (5).** Synthesized from 0.500 g of **1** (1.60 mmol), 0.56 mL of *N,N*-diethylaniline (3.51 mmol), and 0.342 g of *p*-toluidine (3.19 mmol) in 10 mL of dichloromethane, stirring 3 h to yield 0.651 g of crude **5** (90% yield) as a red solid. Dichloromethane was also used instead of ethyl acetate for the first wash: mp > 270 °C; ^1H NMR ($\text{DMSO}-d_6$) δ 10.64 (s, 2 H), 9.08 (s, 2 H), 7.61–7.82 (m, 4 H), 7.18–7.26 (m, 4 H), 2.28 (s, 6H); ^{13}C NMR ($\text{DMSO}-d_6$) δ 160.2, 136.3, 130.1, 129.6, 126.9, 21.4.

***N,N'*-Di-4-methoxyphenyl-5,10-dioxo-5*H*,10*H*-diimidazo[1,5-*a*:1'-5'-*d*]pyrazine-1,6-dicarboxamide (6).** Synthesized from 0.500 g of **1** (1.60 mmol), 0.56 mL of *N,N*-diethylaniline (3.51 mmol), and 0.392 g of *p*-anisidine (3.19 mmol) in 10 mL of dichloromethane, stirring 3 h to yield 0.792 g of crude **6** (102% yield) as a violet solid. Dichloromethane was also used instead of ethyl acetate for the first wash: mp > 270 °C; ^1H NMR ($\text{DMSO}-d_6$) δ 9.11 (s, 2 H), 8.20 (s, 2 H), 7.61–7.72 (m, 4 H), 6.92–7.00 (m, 4 H), 3.75 (s, 6H); ^{13}C NMR ($\text{DMSO}-d_6$) δ 159.0, 135.3, 129.4, 113.8, 113.7, 55.1.

***N,N'*-Di-4-(ethoxycarbonyl)phenyl-5,10-dioxo-5*H*,10*H*-diimidazo[1,5-*a*:1'-5'-*d*]pyrazine-1,6-dicarboxamide (7).** Synthesized from 0.500 g of **1** (1.60 mmol), 0.56 mL of *N,N*-diethylaniline (3.51 mmol), and 0.528 g of ethyl 4-aminobenzoate (3.19 mmol) in 10 mL of dichloromethane, stirring 3 h to yield 0.848 g of crude **7** (95% yield) as a tan solid. Dichloromethane was also used instead of ethyl acetate for the first wash: mp 262–266 °C (dec); ^1H NMR ($\text{DMSO}-d_6$) δ 9.16 (s, 2 H), 8.35 (s, 2 H), 7.95–8.07 (m, 4 H), 4.32–4.36 (m, 4 H), 1.35–1.39 (m, 6H); ^{13}C NMR ($\text{DMSO}-d_6$) δ 165.1, 159.2, 141.7, 135.4, 130.0, 128.5, 120.3, 60.5, 14.1.

***N,N'*-Diphenyl-5,10-dioxo-5*H*,10*H*-diimidazo[1,5-*a*:1'-5'-*d*]pyrazine-1,6-dicarboxamide (8).** Synthesized from 0.500 g of **1** (1.60 mmol), 0.56 mL of *N,N*-diethylaniline (3.51 mmol), and 290 μL of aniline (3.19 mmol) in 10 mL of dichloromethane, stirring 3 h to yield 0.695 g of crude **8** (102% yield) as an orange solid. Dichloromethane was also used instead of ethyl acetate for the first wash: mp 250–254 °C (dec); ^1H NMR ($\text{DMSO}-d_6$) δ 10.48 (s, 2 H), 8.88, 8.85 (s, 2 H), 7.51–7.56 (m,

4 H), 7.14–7.18 (m, 4 H), 6.90–6.95 (m, 2 H); ^{13}C NMR (DMSO- d_6) δ 128.9, 120.0.

***N,N'*-Disubstituted-imidazole-4,5-dicarboxamides (9–36). General Procedure.** To a round-bottom flask was suspended an aniline-substituted pyrazine in ethyl acetate. To this stirred suspension was added all at once a solution of a free amine in ethyl acetate. The free amine, in the case of the amino acid ester salts, was obtained by extraction with a stoichiometric amount of 5 M KOH. The extracted ethyl acetate layer was washed with brine and dried over anhydrous MgSO_4 . The reaction mixture was stirred at room temperature 14–60 h. In most cases the product was purified on SiO_2 with ethyl acetate/hexanes as the eluant.

1*H*-Imidazole-4,5-dicarboxylic Acid 5-[(3,4-Dichlorophenyl)amide] 4-(2-Methylpropyl)amide (9). Synthesized from 65 mg of **2** (0.12 mmol) and 34 μL of isobutylamine (0.35 mmol) in 2 mL of ethyl acetate, stirring the reaction mixture for 60 h. The product was purified by column chromatography on SiO_2 with ethyl acetate as the eluant to yield 11 mg of **9** (13% yield) as a white solid: mp 192–195 °C; TLC R_f (ethyl acetate/hexane 1:1) = 0.35; HPLC (method A) 12.4 min; Intramolecular hydrogen bonded conformational isomers are observed in the ^1H NMR spectrum. ^1H NMR (CDCl_3) δ 13.76 (s, 0.7 H), 12.02 (bs, 0.3 H), 11.73 (bs, 0.7 H), 10.84 (t, J = 6.0 Hz, 0.3 H), 9.51 (s, 0.3 H), 8.13 (s, 0.7 H), 7.96 (s, 0.3 H), 7.82 (t, J = 6.0 Hz, 0.7 H), 7.40–7.68 (m, 3 H), 3.31–3.37 (m, 2 H), 1.90–2.03 (m, 1 H), 1.02–1.06 (m, 6 H); ^{13}C NMR (CDCl_3) δ 163.6, 157.0, 137.9, 136.9, 135.2, 133.8, 132.8, 130.5, 128.5, 127.6, 122.0, 119.7, 46.9, 28.6, 20.4, 20.2; MALDI HR–FTMS calcd for $\text{C}_{15}\text{H}_{16}\text{O}_2\text{N}_4\text{Cl}_2\text{Na}$ m/z 377.0543 [M + Na] $^+$, found 377.0552 [M + Na] $^+$.

1*H*-Imidazole-4,5-dicarboxylic Acid 4-Cyclohexylamide 5-[(3,4-Dichlorophenyl)amide] (10). Synthesized from 79 mg of **2** (0.14 mmol) and 40 μL of cyclohexylamine (0.35 mmol) in 2 mL of ethyl acetate, stirring the reaction mixture for 14 h. The solids were dissolved with methanol and heat. The off-white solid obtained following crystallization was recrystallized from ethyl acetate and methanol. Vacuum filtration gave 46 mg of **10** (43% yield) as an amorphous white solid: mp 235–237 °C; TLC R_f (ethyl acetate/hexane 1:1) = 0.41; HPLC (method B) 14.4 min; ^1H NMR (DMSO- d_6) δ 13.50 (bs, 1 H), 8.75 (bs, 1 H), 8.12 (s, 1 H), 7.95 (s, 1 H), 7.60–7.66 (m, 2 H), 3.78–3.90 (m, 1 H), 1.78–1.88 (m, 2 H), 1.67–1.76 (m, 2 H), 1.55–1.63 (m, 1 H), 1.28–1.47 (m, 4 H), 1.12–1.24 (m, 1 H); ^{13}C NMR (DMSO- d_6) δ 138.5, 136.0, 131.1, 130.8, 125.3, 123.0, 122.5, 47.8, 31.9, 25.0, 24.5; MALDI HR–FTMS calcd for $\text{C}_{17}\text{H}_{18}\text{O}_2\text{N}_4\text{Cl}_2\text{Na}$ m/z 403.0699 [M + Na] $^+$, found 403.0707 [M + Na] $^+$.

1*H*-Imidazole-4,5-dicarboxylic Acid 5-[(3,4-Dichlorophenyl)amide] 4-*n*-Hexylamide (11). Synthesized from 94 mg of **2** (0.17 mmol) and 55 μL of 1-hexylamine (0.42 mmol) in 2 mL of ethyl acetate, stirring the reaction mixture for 16 h. The product was purified by column chromatography on SiO_2 with ethyl acetate/hexanes as the eluant to yield 84 mg of **11** (65% yield) as a white solid: mp 143–146 °C; TLC R_f (ethyl acetate/hexane 1:1) = 0.49; HPLC (method A) 15.3 min; Intramolecular hydrogen bonded conformational isomers are observed in the ^1H NMR spectrum. ^1H NMR (CDCl_3) δ 13.85 (s, 0.8 H), 12.82 (bs, 0.2 H), 12.69 (bs, 0.8 H), 10.86–10.88 (m, 0.2 H), 9.51 (s, 0.2 H), 8.12 (s, 0.8 H), 7.96 (s, 0.2 H), 7.75–7.78 (m, 0.8 H), 7.60–7.62 (m, 1 H), 7.32–7.45 (m, 2 H), 3.40–3.49 (m, 2 H), 1.62–1.68 (m, 2 H), 1.26–1.41 (m, 6 H), 0.89–0.92 (m, 3 H); ^{13}C NMR (CDCl_3) δ 163.4, 161.7, 157.1, 137.9, 137.8, 134.0, 132.6, 129.6, 128.3, 127.9, 127.5, 121.7, 39.7, 31.5, 29.4, 22.6, 14.5, 13.5; MALDI HR–FTMS calcd for $\text{C}_{17}\text{H}_{20}\text{O}_2\text{N}_4\text{Cl}_2\text{Na}$ m/z 405.0856 [M + Na] $^+$, found 405.0847 [M + Na] $^+$.

1*H*-Imidazole-4,5-dicarboxylic Acid 4-Benzylamide 5-[(3,4-Dichlorophenyl)amide] (12). Synthesized from 64 mg of **2** (0.11 mmol) and 37 μL of benzylamine (0.34 mmol) in 2 mL of ethyl acetate, stirring the reaction mixture for 18 h. The product was purified by column chromatography on SiO_2 with ethyl acetate as the eluant to yield 17 mg of **12** (19% yield) as a white solid: mp 204–205 °C; TLC R_f (ethyl acetate/hexane 1:1) = 0.53; HPLC (method A) 11.9 min; Intramolecular

hydrogen bonded conformational isomers are observed in the ^1H NMR spectrum. ^1H NMR (CDCl_3) δ 13.66 (s, 0.7 H), 12.12 (bs, 0.3 H), 11.65 (bs, 0.7 H), 11.33–11.37 (m, 0.3 H), 9.49 (s, 0.3 H), 8.12 (s, 0.7 H), 8.02–8.09 (m, 0.7 H), 7.94 (m, 0.3 H), 7.55–7.62 (m, 2 H), 7.31–7.43 (m, 6 H), 4.68–4.71 (m, 2 H); ^{13}C NMR (CDCl_3) δ 163.5, 156.8, 137.8, 137.3, 133.5, 130.6, 128.9, 128.7, 127.9, 127.8, 127.5, 122.0, 43.5; MALDI HR–FTMS calcd for $\text{C}_{18}\text{H}_{14}\text{O}_2\text{N}_4\text{Cl}_2\text{Na}$ m/z 411.0386 [M + Na] $^+$, found 411.0388 [M + Na] $^+$.

1*H*-Imidazole-4,5-dicarboxylic Acid 5-[(3,4-Dichlorophenyl)amide] 4-Phenethylamide (13). Synthesized from 74 mg of **2** (0.13 mmol) and 41 μL of phenethylamine (0.33 mmol) in 2 mL of ethyl acetate, stirring the reaction mixture for 16 h. The product was purified by column chromatography on SiO_2 with ethyl acetate as the eluant to yield 41 mg of **13** (38% yield) as a white solid: mp 187–190 °C; TLC R_f (ethyl acetate/hexane 1:1) = 0.54; HPLC (method A) 12.5 min; Intramolecular hydrogen bonded conformational isomers are observed in the ^1H NMR spectrum. ^1H NMR (CDCl_3) δ 13.70 (s, 0.7 H), 12.50 (bs, 0.3 H), 12.25 (bs, 0.7 H), 10.89–10.91 (m, 0.3 H), 9.40 (s, 0.3 H), 8.06 (s, 0.7 H), 7.95 (s, 0.3 H), 7.75–7.78 (m, 0.7 H), 7.55–7.56 (m, 1 H), 7.16–7.33 (m, 7 H), 3.63–3.71 (m, 2 H), 2.87–2.94 (m, 2 H); ^{13}C NMR (CDCl_3) δ 163.6, 161.6, 158.6, 157.1, 138.5, 137.8, 136.8, 133.8, 133.0, 132.7, 129.5, 129.2, 129.0, 128.5, 128.3, 128.0, 127.6, 121.9, 121.8, 40.8, 35.7; MALDI HR–FTMS calcd for $\text{C}_{19}\text{H}_{16}\text{O}_2\text{N}_4\text{Cl}_2\text{Na}$ m/z 425.0543 [M + Na] $^+$, found 425.0533 [M + Na] $^+$.

1*H*-Imidazole-4,5-dicarboxylic Acid 4-Chlorobenzylamide 5-[(3,4-Dichlorophenyl)amide] (14). Synthesized from 110 mg of **2** (0.20 mmol) and 53 μL of 4-chlorobenzylamine (0.43 mmol) in 2 mL of ethyl acetate, stirring the reaction mixture for 16 h. The product solid was collected by vacuum filtration and washed with ethyl acetate. Crystallization from ethyl acetate/methanol provided 85 mg of **14** (52% yield) as a white solid: mp 218–219 °C; TLC R_f (ethyl acetate/hexane 1:1) = 0.47; HPLC (method B) 13.0 min; ^1H NMR (DMSO- d_6) δ 13.82 (bs, 1 H), 9.53 (bs, 1 H), 8.08 (bs, 1 H), 7.98 (s, 1 H), 7.34–7.62 (m, 7 H), 4.52–4.53 (m, 2 H); ^{13}C NMR (DMSO- d_6) δ 137.9, 133.5, 133.1, 131.4, 130.7, 129.1, 128.5, 128.3, 43.8; MALDI HR–FTMS calcd for $\text{C}_{18}\text{H}_{12}\text{O}_2\text{N}_4\text{Cl}_3\text{Na}$ m/z 444.9996 [M + Na] $^+$, found 444.9998 [M + Na] $^+$.

1*H*-Imidazole-4,5-dicarboxylic Acid 5-[(3,4-Dichlorophenyl)amide] 4-Methylbenzylamide (15). Synthesized from 90 mg of **2** (0.16 mmol) and 45 μL of 4-methylbenzylamine (0.35 mmol) in 2 mL of ethyl acetate, stirring the reaction mixture for 16 h. The product solid was collected by vacuum filtration and washed with ethyl acetate. Crystallization from ethyl acetate/methanol provided 55 mg of **15** (43% yield) as a white solid: mp 213–225 °C (dec); TLC R_f (ethyl acetate/hexane 1:1) = 0.55; HPLC (method A) 13.0 min; ^1H NMR (DMSO- d_6) δ 13.90 (s, 1 H), 9.20 (s, 1 H), 8.04–8.06 (m, 1 H), 7.98 (s, 1 H), 7.05–7.66 (m, 7 H), 4.49–4.51 (m, 2 H), 2.07 (s, 3 H); ^{13}C NMR (DMSO- d_6) δ 137.8, 135.9, 135.7, 135.3, 130.9, 129.1, 129.0, 128.8, 128.7, 127.7, 127.1, 42.0; MALDI HR–FTMS calcd for $\text{C}_{19}\text{H}_{16}\text{O}_2\text{N}_4\text{Cl}_2\text{Na}$ m/z 425.0543 [M + Na] $^+$, found 425.0545 [M + Na] $^+$.

1*H*-Imidazole-4,5-dicarboxylic Acid 5-[(3,4-Dichlorophenyl)amide] 4-Methoxybenzylamide (16). Synthesized from 89 mg of **2** (0.16 mmol) and 51 μL of 4-methoxybenzylamine (0.39 mmol) in 2 mL of ethyl acetate, stirring the reaction mixture for 16 h. The product solid was collected by vacuum filtration. Crystallization from ethyl acetate/methanol provided 87 mg of **16** (66% yield) as a white solid: mp 208–209 °C; TLC R_f (ethyl acetate/hexane 1:1) = 0.37; HPLC (method A) 11.5 min; ^1H NMR (DMSO- d_6) δ 13.90 (bs, 1 H), 10.60 (bs, 1 H), 9.45 (bs, 1 H), 8.12 (s, 1 H), 7.98 (s, 1 H), 7.56–7.62 (m, 2 H), 7.28–7.30 (m, 1 H), 6.89–6.99 (s, 1 H), 7.48–7.50 (m, 2 H), 3.72, 3.76 (s, 3 H); ^{13}C NMR (DMSO- d_6) δ 159.1, 158.1, 135.2, 130.6, 130.1, 128.5, 126.0, 113.7, 113.5, 59.5, 55.0, 54.8, 20.5, 13.8; MALDI HR–FTMS calcd for $\text{C}_{19}\text{H}_{16}\text{O}_3\text{N}_4\text{Cl}_2\text{Na}$ m/z 441.0492 [M + Na] $^+$, found 441.0497 [M + Na] $^+$.

1*H*-Imidazole-4,5-dicarboxylic Acid 5-[(3,4-Dichlorophenyl)amide] 4-Phenylbenzylamide (17). Synthesized from 79 mg of **2** (0.14 mmol) and 54 mg of 4-phenylbenzyl-

amine (0.30 mmol) in 2 mL of ethyl acetate, stirring the reaction mixture for 16 h. The product solid was collected by vacuum filtration and washed with ethyl acetate to provide 61 mg of **17** (47% yield) as a white solid: mp 242–244 °C; TLC R_f (ethyl acetate/hexane 1:1) = 0.58; HPLC (method A) 14.3 min; Intramolecular hydrogen bonded conformational isomers are observed in the ^1H NMR spectrum. ^1H NMR (DMSO- d_6) δ 13.90 (bs, 0.7 H), 13.59 (bs, 1 H), 9.53 (bs, 0.7 H), 8.89 (s, 0.3 H), 8.11 (m, 0.7 H), 8.00 (s, 1 H), 7.33–7.65 (m, 12 H), 4.60–4.62 (m, 2 H); ^{13}C NMR (DMSO- d_6) δ 139.9, 138.9, 138.1, 128.9, 127.9, 127.3, 126.7, 126.6, 42.0; MALDI HR–FTMS calcd for $\text{C}_{24}\text{H}_{18}\text{O}_2\text{N}_4\text{Cl}_2\text{Na}$ m/z 487.0699 [M + Na] $^+$, found 487.0703 [M + Na] $^+$.

(R)-1H-Imidazole-4,5-dicarboxylic Acid 5-[(3,4-Dichlorophenyl)amide] 4-[(1-Phenylethyl)amide] (18). Synthesized from 46 mg of **2** (0.08 mmol) and 23 μL of (*R*)- α -methylbenzylamine (0.18 mmol) in 2 mL of ethyl acetate, stirring the reaction mixture for 16 h. The product was purified by column chromatography on SiO_2 with ethyl acetate as the eluant to yield 42 mg of **18** (64% yield) as a white solid: mp 196–199 °C; TLC R_f (ethyl acetate/hexane 1:1) = 0.28; HPLC (method A) 12.6 min; Intramolecular hydrogen bonded conformational isomers are observed in the ^1H NMR spectrum. ^1H NMR (CDCl_3) δ 13.72 (s, 0.7 H), 12.70 (bs, 0.3 H), 12.32 (bs, 0.7 H), 11.43–11.44 (m, 0.3 H), 9.53 (s, 0.3 H), 8.12 (s, 0.7 H), 7.97–8.02 (m, 1 H), 7.25–7.50 (m, 8 H), 5.29–5.35 (m, 0.7 H), 5.19–5.22 (m, 0.3 H), 1.63–1.67 (m, 3 H); ^{13}C NMR (CDCl_3) δ 162.8, 161.8, 158.1, 157.1, 142.5, 137.8, 136.8, 133.8, 133.0, 132.7, 130.7, 130.5, 129.4, 128.9, 128.7, 128.0, 127.7, 126.0, 122.0, 119.7, 50.4, 49.0, 23.0, 22.4; MALDI HR–FTMS calcd for $\text{C}_{19}\text{H}_{16}\text{O}_2\text{N}_4\text{Cl}_2\text{Na}$ m/z 425.0543 [M + Na] $^+$, found 525.0534 [M + Na] $^+$.

(S)-1H-Imidazole-4,5-dicarboxylic Acid 5-[(3,4-Dichlorophenyl)amide] 4-[(1-Phenylethyl)amide] (19). Synthesized from 55 mg of **2** (0.10 mmol) and 27 μL of (*S*)- α -methylbenzylamine (0.22 mmol) in 2 mL of ethyl acetate, stirring the reaction mixture for 16 h. The product was purified by column chromatography on SiO_2 with ethyl acetate as the eluant to yield 43 mg of **19** (55% yield) as a white solid: Physical and spectral data identical to enantiomer **18**.

2-[[5-(3,4-Dichlorophenylcarbamoyl)-1H-imidazole-4-carbonyl]amino]ethanoic Acid *tert*-Butyl Ester (20). Synthesized from 62 mg of **2** (0.11 mmol) and 55 mg of glycine *tert*-butyl ester hydrochloride (0.33 mmol, neutralized) in 2 mL of ethyl acetate, stirring the reaction mixture for 18 h. The product was purified by column chromatography on SiO_2 with ethyl acetate as the eluant to yield 14 mg of **20** (15% yield) as a white solid: mp 212–213 °C; TLC R_f (ethyl acetate/hexane 1:1) = 0.32; HPLC (method A) 11.6 min; Intramolecular hydrogen bonded conformational isomers are observed in the ^1H NMR spectrum. ^1H NMR (CDCl_3) δ 13.44 (s, 0.7 H), 12.00 (bs, 0.3 H), 11.67 (bs, 0.7 H), 11.20–11.23 (m, 0.3 H), 9.50 (s, 0.3 H), 8.13–8.16 (m, 0.7 H), 8.08 (s, 0.7 H), 8.00 (s, 0.3 H), 7.26–7.69 (m, 3 H), 4.15–4.18 (m, 2 H), 1.52, 1.53 (s, 9 H); ^{13}C NMR (CDCl_3) δ 168.5, 164.0, 138.2, 135.4, 133.1, 130.9, 129.2, 128.0, 124.1, 122.2, 119.9, 83.2, 42.4, 28.5; MALDI HR–FTMS calcd for $\text{C}_{17}\text{H}_{18}\text{O}_4\text{N}_4\text{Cl}_2\text{Na}$ m/z 435.0597 [M + Na] $^+$, found 435.0588 [M + Na] $^+$.

(R)-2-[[5-(3,4-Dichlorophenylcarbamoyl)-1H-imidazole-4-carbonyl]amino]propionic Acid Methyl Ester (21). Synthesized from 74 mg of **2** (0.13 mmol) and 56 mg of (*R*)-alanine methyl ester hydrochloride (0.33 mmol, neutralized) in 2 mL of ethyl acetate, stirring the reaction mixture for 16 h. The product was purified by column chromatography on SiO_2 with ethyl acetate as the eluant to yield 36 mg of **21** (36% yield) as a white solid: mp 186–190 °C; TLC R_f (ethyl acetate/hexane 1:1) = 0.18; HPLC (method A) 9.3 min; Intramolecular hydrogen bonded conformational isomers are observed in the ^1H NMR spectrum. ^1H NMR (CDCl_3) δ 13.47 (s, 0.7 H), 12.48 (bs, 0.3 H), 12.16 (bs, 0.7 H), 11.35 (d, J = 8.0 Hz, 0.3 H), 9.52 (s, 0.3 H), 8.18 (d, J = 8.0 Hz, 0.7 H), 8.10 (s, 0.7 H), 7.96 (s, 0.3 H), 7.26–7.70 (m, 3 H), 4.65–4.88 (m, 2 H), 3.79, 3.82 (s, 3 H), 1.58–1.65 (m, 3 H); ^{13}C NMR (CDCl_3) δ 172.8, 172.6, 163.2, 161.6, 156.9, 137.7, 136.7, 135.6, 133.5, 133.2, 133.0,

132.8, 130.6, 130.5, 128.9, 128.7, 128.1, 127.7, 121.9, 121.8, 119.6, 119.4, 52.7, 52.5, 49.1, 48.2, 18.3, 17.6; MALDI HR–FTMS calcd for $\text{C}_{15}\text{H}_{14}\text{O}_4\text{N}_4\text{Cl}_2\text{Na}$ m/z 407.0284 [M + Na] $^+$, found 407.0290 [M + Na] $^+$.

(R)-2-[[5-(3,4-Dichlorophenylcarbamoyl)-1H-imidazole-4-carbonyl]amino]propionic Acid *tert*-Butyl Ester (22). Synthesized from 81 mg of **2** (0.14 mmol) and 83 mg of (*R*)-alanine *tert*-butyl ester hydrochloride (0.46 mmol, neutralized) in 2 mL of ethyl acetate, stirring the reaction mixture for 16 h. The product was purified by column chromatography on SiO_2 with ethyl acetate/hexanes as the eluant to yield 33 mg of **22** (27% yield) as a white solid: mp 189–191 °C; TLC R_f (ethyl acetate/hexane 1:1) = 0.45; HPLC (method A) 12.8 min; Intramolecular hydrogen bonded conformational isomers are observed in the ^1H NMR spectrum. ^1H NMR (CDCl_3) δ 13.57 (s, 0.8 H), 12.42 (bs, 0.2 H), 12.11 (bs, 0.8 H), 11.30 (d, J = 8.0 Hz, 0.2 H), 9.55 (s, 0.2 H), 8.21 (d, J = 8.0 Hz, 0.8 H), 8.10 (s, 0.8 H), 7.96 (s, 0.2 H), 7.26–7.70 (m, 3 H), 4.63–4.66 (m, 1.6 H), 4.08–4.11 (m, 0.4 H), 1.26–1.60 (m, 12 H); ^{13}C NMR (CDCl_3) δ 171.4, 171.3, 163.2, 161.5, 157.0, 137.8, 136.8, 135.5, 133.5, 133.0, 132.8, 130.6, 130.5, 129.0, 128.8, 127.6, 121.9, 121.8, 119.6, 82.5, 82.0, 48.9, 28.1, 28.0, 18.5; MALDI HR–FTMS calcd for $\text{C}_{18}\text{H}_{20}\text{O}_4\text{N}_4\text{Cl}_2\text{Na}$ m/z 449.0754 [M + Na] $^+$, found 449.0760 [M + Na] $^+$.

(S)-2-[[5-(3,4-Dichlorophenylcarbamoyl)-1H-imidazole-4-carbonyl]amino]propionic Acid *tert*-Butyl Ester (23). Synthesized from 71 mg of **2** (0.13 mmol) and 69 mg of (*S*)-alanine *tert*-butyl ester hydrochloride (0.38 mmol, neutralized) in 2 mL of ethyl acetate, stirring the reaction mixture for 16 h. The product was purified by column chromatography on SiO_2 with ethyl acetate/hexanes as the eluant to yield 14 mg of **23** (13% yield) as a white solid: The physical and spectral data was identical with enantiomer **22**.

(R)-2-[[5-(3,4-Dichlorophenylcarbamoyl)-1H-imidazole-4-carbonyl]amino]phenylethanoic Acid Methyl Ester (24). Synthesized from 82 mg of **2** (0.15 mmol) and 70 mg of (*R*)-phenylglycine methyl ester hydrochloride (0.35 mmol, neutralized) in 2 mL of ethyl acetate, stirring the reaction mixture for 16 h. The product was purified by column chromatography on SiO_2 with ethyl acetate/hexanes as the eluant to yield 27 mg of **24** (23% yield) as a white solid: mp 199–203 °C; TLC R_f (ethyl acetate/hexane 1:1) = 0.37; HPLC (method A) 11.0 min; Intramolecular hydrogen bonded conformational isomers are observed in the ^1H NMR spectrum. ^1H NMR (CDCl_3) δ 13.34 (s, 0.7 H), 12.33 (bs, 0.3 H), 11.97–11.99 (m, 1 H), 9.49 (s, 0.3 H), 8.59 (d, J = 8.0 Hz, 0.7 H), 8.08 (s, 0.7 H), 7.94 (s, 0.3 H), 7.26–7.64 (m, 8 H), 5.74–5.79 (m, 1 H), 3.78, 3.81 (s, 3 H); ^{13}C NMR (CDCl_3) δ 170.7, 170.6, 163.1, 161.5, 156.8, 137.6, 135.8, 133.0, 132.7, 129.0, 128.5, 127.7, 121.9; MALDI HR–FTMS calcd for $\text{C}_{20}\text{H}_{16}\text{O}_4\text{N}_4\text{Cl}_2\text{Na}$ m/z 469.0441 [M + Na] $^+$, found 469.0440 [M + Na] $^+$.

(S)-2-[[5-(3,4-Dichlorophenylcarbamoyl)-1H-imidazole-4-carbonyl]amino]phenylethanoic Acid Methyl Ester (25). Synthesized from 80 mg of **2** (0.14 mmol) and 69 mg of (*S*)-phenylglycine methyl ester hydrochloride (0.34 mmol, neutralized) in 2 mL of ethyl acetate, stirring the reaction mixture for 16 h. The product was purified by column chromatography on SiO_2 with ethyl acetate/hexanes as the eluant to yield 24 mg of **25** (20% yield) as a white solid: The physical and spectral data was identical with enantiomer **24**.

(R)-2-[[5-(3,4-Dichlorophenylcarbamoyl)-1H-imidazole-4-carbonyl]amino]-3-methylbutyric Acid Methyl Ester (26). Synthesized from 77 mg of **2** (0.14 mmol) and 66 mg of (*R*)-valine methyl ester hydrochloride (0.39 mmol, neutralized) in 2 mL of ethyl acetate, stirring the reaction mixture for 16 h. The product was purified by column chromatography on SiO_2 with ethyl acetate/hexanes as the eluant to yield 47 mg of **26** (41% yield) as a white solid: mp 130–135 °C; TLC R_f (ethyl acetate/hexane 1:1) = 0.27; HPLC (method A) 11.4 min; Intramolecular hydrogen bonded conformational isomers are observed in the ^1H NMR spectrum. ^1H NMR (CDCl_3) δ 13.51 (s, 0.7 H), 12.50 (bs, 0.3 H), 12.24 (s, 0.7 H), 11.36 (d, J = 8.0 Hz, 1 H), 9.54 (s, 0.3 H), 8.16 (d, J = 8.0 Hz, 0.7 H), 8.13 (s, 0.7 H), 7.93 (s, 0.3 H), 7.26–7.68 (m, 3 H), 4.70–4.74 (m, 1

H), 3.79, 3.81 (s, 3 H), 2.32–2.45 (m, 1 H), 1.04–1.15 (m, 6 H); ^{13}C NMR (CDCl_3) δ 171.9, 171.7, 163.6, 161.5, 156.9, 137.8, 136.9, 135.5, 133.3, 132.9, 132.8, 130.5, 128.8, 128.0, 127.7, 122.0, 121.8, 119.6, 119.4, 57.4, 52.4, 52.2, 31.4, 19.2, 18.1, 18.0; MALDI HR–FTMS calcd for $\text{C}_{17}\text{H}_{18}\text{O}_4\text{N}_4\text{Cl}_2\text{Na}$ m/z 435.0597 $[\text{M} + \text{Na}]^+$, found 435.0585 $[\text{M} + \text{Na}]^+$.

(S)-2-[[5-(3,4-Dichloro-phenylcarbamoyl)-1H-imidazole-4-carbonyl]-amino]-3-methylbutyric Acid Methyl Ester (27). Synthesized from 81 mg of **2** (0.14 mmol) and 80 mg of (*S*)-valine methyl ester hydrochloride (0.47 mmol, neutralized) in 2 mL of ethyl acetate, stirring the reaction mixture for 16 h. The product was purified by column chromatography on SiO_2 with ethyl acetate/hexanes as the eluant to yield 21 mg of **27** (18% yield) as a white solid: The physical and spectral data was identical with enantiomer **26**.

(R)-2-[[5-(3-Chlorophenylcarbamoyl)-1H-imidazole-4-carbonyl]amino]propionic Acid *tert*-Butyl Ester (28). Synthesized from 43 mg of **3** (0.087 mmol) and 47 mg of (*R*)-alanine *tert*-butyl ester hydrochloride (0.26 mmol, neutralized) in 2 mL of ethyl acetate, stirring the reaction mixture for 16 h. The product was purified by column chromatography on SiO_2 with ethyl acetate/hexanes as the eluant to yield 37 mg of **28** (54% yield) as a white solid: mp 168–171 °C; TLC R_f (ethyl acetate/hexane 1:1) = 0.30; HPLC (method A) 11.2 min; Intramolecular hydrogen bonded conformational isomers are observed in the ^1H NMR spectrum. ^1H NMR (CDCl_3) δ 13.53 (s, 0.7 H), 12.65 (bs, 0.3 H), 12.40 (s, 0.7 H), 11.37 (d, J = 8.0 Hz, 1 H), 9.54 (s, 0.3 H), 8.21 (d, J = 8.0 Hz, 0.7 H), 8.01 (s, 0.7 H), 7.91 (s, 0.3 H), 7.11–7.70 (m, 4 H), 4.58–4.70 (m, 1 H), 1.51–1.60 (m, 12 H); ^{13}C NMR (CDCl_3) δ 171.4, 171.3, 163.2, 161.6, 158.5, 157.1, 139.5, 138.5, 135.6, 135.1, 134.8, 134.6, 133.7, 133.4, 130.0, 128.9, 124.7, 124.5, 120.4, 120.3, 118.4, 118.2, 82.4, 82.0, 49.9, 48.9, 28.1, 28.0, 18.5, 17.9; MALDI HR–FTMS calcd for $\text{C}_{18}\text{H}_{21}\text{O}_4\text{N}_4\text{ClNa}$ m/z 415.1144 $[\text{M} + \text{Na}]^+$, found 415.1144 $[\text{M} + \text{Na}]^+$.

(R)-2-[[5-(4-Chlorophenylcarbamoyl)-1H-imidazole-4-carbonyl]amino]propionic Acid *tert*-Butyl Ester (29). Synthesized from 53 mg of **4** (0.11 mmol) and 58 mg of (*R*)-alanine *tert*-butyl ester hydrochloride (0.32 mmol, neutralized) in 2 mL of ethyl acetate, stirring the reaction mixture for 16 h. The product was purified by column chromatography on SiO_2 with ethyl acetate/hexanes as the eluant to yield 28 mg of **29** (33% yield) as a white solid: mp 174–175 °C; TLC R_f (ethyl acetate/hexane 1:1) = 0.26; HPLC (method A) 11.0 min; Intramolecular hydrogen bonded conformational isomers are observed in the ^1H NMR spectrum. ^1H NMR (CDCl_3) δ 13.47 (s, 0.7 H), 12.46 (bs, 0.3 H), 12.05 (s, 0.7 H), 11.37 (d, J = 8.0 Hz, 1 H), 9.47 (s, 0.3 H), 8.20 (d, J = 8.0 Hz, 0.7 H), 7.65–7.75 (m, 3 H), 7.26–7.34 (m, 2 H), 4.60–4.70 (m, 1 H), 1.51–1.59 (m, 12 H); ^{13}C NMR (CDCl_3) δ 171.4, 171.3, 163.2, 161.6, 158.5, 157.1, 139.5, 138.5, 135.6, 135.1, 134.8, 134.6, 133.7, 133.4, 130.0, 128.9, 124.7, 124.5, 120.4, 120.3, 118.4, 118.2, 82.4, 82.0, 49.9, 48.9, 28.1, 28.0, 18.5, 17.9; MALDI HR–FTMS calcd for $\text{C}_{18}\text{H}_{21}\text{O}_4\text{N}_4\text{ClNa}$ m/z 415.1144 $[\text{M} + \text{Na}]^+$, found 415.1155 $[\text{M} + \text{Na}]^+$.

(R)-2-[[5-(4-Methylphenylcarbamoyl)-1H-imidazole-4-carbonyl]amino]propionic Acid *tert*-Butyl Ester (30). Synthesized from 90 mg of **5** (0.20 mmol) and 90 mg of (*R*)-alanine *tert*-butyl ester hydrochloride (0.50 mmol, neutralized) in 3 mL of ethyl acetate, stirring the reaction mixture for 24 h. The product was purified by column chromatography on SiO_2 with ethyl acetate/hexanes as the eluant to yield 65 mg of **30** (46% yield) as a white solid: mp 165–168 °C; TLC R_f (ethyl acetate/hexane 1:1) = 0.67; HPLC (method A) 10.2 min; Intramolecular hydrogen bonded conformational isomers are observed in the ^1H NMR spectrum. ^1H NMR (CDCl_3) δ 13.35 (s, 0.7 H), 12.80 (bs, 0.3 H), 12.67 (s, 0.7 H), 11.58 (d, J = 8.0 Hz, 1 H), 9.47 (s, 0.3 H), 8.21 (d, J = 8.0 Hz, 0.7 H), 7.66–7.70 (m, 3 H), 7.17–7.19 (m, 2 H), 4.61–4.71 (m, 1 H), 2.35, 2.34 (s, 3 H), 1.50–1.59 (m, 12 H); ^{13}C NMR (CDCl_3) δ 171.5, 171.4, 163.3, 161.4, 158.8, 156.8, 135.7, 134.4, 134.2, 134.1, 133.0, 130.1, 129.7, 129.3, 129.0, 128.5, 120.5, 120.4, 120.3, 120.2, 82.2, 81.7, 49.2, 48.4, 28.7, 28.6, 28.2, 27.5, 21.1, 19.1, 18.3,

17.9, 17.2; MALDI HR–FTMS calcd for $\text{C}_{19}\text{H}_{24}\text{O}_4\text{N}_4\text{Na}$ m/z 395.1690 $[\text{M} + \text{Na}]^+$, found 395.1700 $[\text{M} + \text{Na}]^+$.

(R)-2-[[5-(4-Methoxyphenylcarbamoyl)-1H-imidazole-4-carbonyl]amino]propionic Acid *tert*-Butyl Ester (31). Synthesized from 99 mg of **6** (0.20 mmol) and 92 mg of (*R*)-alanine *tert*-butyl ester hydrochloride (0.51 mmol, neutralized) in 3 mL of ethyl acetate, stirring the reaction mixture for 24 h. The product was purified by column chromatography on SiO_2 with ethyl acetate/hexanes as the eluant to yield 90 mg of **31** (58% yield) as a white solid: mp 146–151 °C; TLC R_f (ethyl acetate/hexane 1:1) = 0.58; HPLC (method A) 8.5 min; Intramolecular hydrogen bonded conformational isomers are observed in the ^1H NMR spectrum. ^1H NMR (CDCl_3) δ 13.21 (s, 0.7 H), 12.79 (bs, 0.3 H), 12.67 (s, 0.7 H), 11.55 (d, J = 8.0 Hz, 1 H), 9.35 (s, 0.3 H), 8.15 (d, J = 8.0 Hz, 0.7 H), 7.52–7.65 (m, 3 H), 6.81–6.84 (m, 2 H), 4.55–4.65 (m, 1 H), 3.73, 3.72 (s, 3 H), 1.40–1.51 (m, 12 H); ^{13}C NMR (CDCl_3) δ 171.5, 171.4, 163.3, 161.7, 161.3, 158.8, 156.6, 156.5, 134.1, 133.0, 131.5, 131.4, 130.4, 129.4, 128.4, 122.1, 121.9, 121.8, 121.7, 114.8, 114.7, 113.9, 113.5, 82.2, 82.2, 81.7, 56.1, 55.8, 55.7, 55.2, 55.1, 54.8, 54.6, 49.2, 48.3, 28.6, 28.2, 27.8, 27.3, 18.3, 17.8; MALDI HR–FTMS calcd for $\text{C}_{19}\text{H}_{24}\text{O}_5\text{N}_4\text{Na}$ m/z 411.1639 $[\text{M} + \text{Na}]^+$, found 411.1651 $[\text{M} + \text{Na}]^+$.

(R)-4-[[5-(1-*tert*-Butoxycarbonyl-ethylcarbamoyl)-3H-imidazole-4-carbonyl]amino]benzoic Acid Ethyl Ester (32). Synthesized from 83 mg of **7** (0.15 mmol) and 67 mg of (*R*)-alanine *tert*-butyl ester hydrochloride (0.37 mmol, neutralized) in 3 mL of ethyl acetate, stirring the reaction mixture for 24 h. The product was purified by column chromatography on SiO_2 with ethyl acetate/hexanes as the eluant to yield 62 mg of **32** (48% yield) as a white solid: mp 128–130 °C; TLC R_f (ethyl acetate/hexane 1:1) = 0.62; HPLC (method A) 10.4 min; Intramolecular hydrogen bonded conformational isomers are observed in the ^1H NMR spectrum. ^1H NMR (CDCl_3) δ 13.67 (s, 0.7 H), 12.77 (bs, 0.3 H), 12.45 (s, 0.7 H), 11.40 (d, J = 8.0 Hz, 1 H), 9.71 (s, 0.3 H), 8.25 (d, J = 8.0 Hz, 0.7 H), 8.04–8.07 (m, 2 H), 7.82–7.87 (m, 2 H), 7.69–7.70 (m, 1 H), 4.62–4.72 (m, 1 H), 4.35–4.41 (m, 2 H), 1.52–1.61 (m, 9 H), 1.38–1.43 (m, 3 H); ^{13}C NMR (CDCl_3) δ 171.5, 171.3, 166.2, 166.1, 163.2, 161.6, 158.4, 157.2, 142.4, 141.4, 133.6, 133.3, 130.8, 130.7, 128.9, 126.3, 126.1, 119.5, 82.2, 82.3, 60.9, 28.6, 28.2, 27.7, 27.3, 17.8; MALDI HR–FTMS calcd for $\text{C}_{18}\text{H}_{22}\text{O}_4\text{N}_4\text{Na}$ m/z 381.1533 $[\text{M} + \text{Na}]^+$, found 381.1531 $[\text{M} + \text{Na}]^+$.

(R)-2-[[5-(phenylcarbamoyl)-1H-imidazole-4-carbonyl]-amino]propionic Acid *tert*-Butyl Ester (33). Synthesized from 65 mg of **8** (0.15 mmol) and 69 mg of (*R*)-alanine *tert*-butyl ester hydrochloride (0.38 mmol, neutralized) in 3 mL of ethyl acetate, stirring the reaction mixture for 24 h. The product was purified by column chromatography on SiO_2 with ethyl acetate/hexanes as the eluant to yield 74 mg of **33** (67% yield) as a white solid: mp 166–169 °C; TLC R_f (ethyl acetate/hexane 1:1) = 0.66; HPLC (method A) 9.2 min; Intramolecular hydrogen bonded conformational isomers are observed in the ^1H NMR spectrum. ^1H NMR (CDCl_3) δ 13.42 (s, 0.7 H), 12.93 (bs, 0.3 H), 12.75 (s, 0.7 H), 11.58 (d, J = 8.0 Hz, 1 H), 9.55 (s, 0.3 H), 8.26 (d, J = 8.0 Hz, 0.7 H), 7.67–7.82 (m, 3 H), 7.15–7.40 (m, 3 H), 4.65–4.74 (m, 1 H), 1.49–1.60 (m, 9 H), 1.38–1.43 (m, 3 H); ^{13}C NMR (CDCl_3) δ 171.5, 171.4, 163.3, 161.5, 158.7, 157.0, 138.2, 137.2, 134.0, 133.2, 129.4, 129.2, 128.8, 128.6, 120.4, 120.3, 82.2, 81.8, 49.2, 48.4, 28.6, 28.2, 27.8, 27.3, 18.3, 17.8; MALDI HR–FTMS calcd for $\text{C}_{21}\text{H}_{26}\text{O}_6\text{N}_4\text{Na}$ m/z 453.1745 $[\text{M} + \text{Na}]^+$, found 453.1751 $[\text{M} + \text{Na}]^+$.

1H-Imidazole-4,5-dicarboxylic Acid 5-[[3,4-Dichlorophenylamide] 4-Di-*n*-propylamide (34). Synthesized from 64 mg of **2** (0.11 mmol) and 47 μL of di-*n*-propylamine (0.34 mmol) in 2 mL of ethyl acetate, stirring the reaction mixture for 48 h. The product was purified by column chromatography on SiO_2 with ethyl acetate/hexanes as the eluant to yield 21 mg of **34** (25% yield) as a white solid: mp 163–166 °C; TLC R_f (ethyl acetate/hexane 1:1) = 0.52; HPLC (method A) 12.7 min; ^1H NMR (CDCl_3) δ 13.22 (s, 1 H), 11.68 (s, 1 H), 8.10 (s, 1 H), 7.28–7.72 (m, 3 H), 3.87–3.91 (m, 2 H), 3.51–3.55 (m, 2 H), 1.69–1.77 (m, 4 H), 0.87–1.04 (m, 6 H); ^{13}C NMR (CDCl_3) δ 165.1, 157.6, 137.9, 135.6, 134.4, 132.7, 130.5, 129.9, 127.5,

122.0, 119.7, 51.4, 49.6, 22.5, 20.8, 11.6, 11.1; MALDI HR-FTMS calcd for $C_{17}H_{20}O_2N_4Cl_2Na$ m/z 405.0856 $[M + Na]^+$, found 405.0856 $[M + Na]^+$.

(R)-1H-Imidazole-4,5-dicarboxylic Acid 5-[(3,4-Dichlorophenyl)amide] 4-[Methyl(1-phenylethyl)amide] (35). Synthesized from 76 mg of **2** (0.13 mmol) and 78 μ L of (*R*)-*N*, α -dimethylbenzylamine (0.54 mmol) in 2 mL of ethyl acetate, stirring the reaction mixture for 60 h. The product was purified by column chromatography on SiO_2 with ethyl acetate/hexanes as the eluant to yield 35 mg of **35** (31% yield) as a white solid: mp 186–188 °C; TLC R_f (ethyl acetate/hexane 1:1) = 0.27; HPLC (method A) 11.9 min; Conformational isomers are observed in the 1H NMR spectrum. 1H NMR ($CDCl_3$) δ 13.30 (s, 0.5 H), 13.18 (s, 0.5 H), 12.09 (s, 1 H), 8.16 (s, 0.5 H), 8.16 (s, 0.5 H), 7.28–7.76 (m, 3 H), 6.82–6.84 (m, 0.5 H), 6.22–6.24 (m, 0.5 H), 3.17 (s, 1.5 H), 2.84 (s, 1.5 H), 1.67–1.79 (m, 3 H); ^{13}C NMR ($CDCl_3$) δ 165.6, 165.4, 157.6, 140.1, 139.7, 137.8, 135.5, 132.8, 130.6, 130.3, 130.2, 128.7, 128.6, 127.7, 127.6, 127.5, 127.4, 127.1, 122.0, 121.9, 119.6, 60.4, 55.8, 52.6, 32.6, 29.5, 21.1, 17.0, 15.6; MALDI HR-FTMS calcd for $C_{20}H_{18}O_2N_4Cl_2Na$ m/z 439.0699 $[M + Na]^+$, found 439.0706 $[M + Na]^+$.

(S)-1H-Imidazole-4,5-dicarboxylic Acid 5-[(3,4-Dichlorophenyl)amide] 4-[Methyl(1-phenylethyl)amide] (36). Synthesized from 72 mg of **2** (0.13 mmol) and 75 μ L of (*R*)-*N*, α -dimethylbenzylamine (0.51 mmol) in 2 mL of ethyl acetate, stirring the reaction mixture for 60 h. The product was purified by column chromatography on SiO_2 with ethyl acetate/hexanes as the eluant to yield 38 mg of **36** (36% yield) as a white solid: The physical and spectral data was identical with enantiomer **35**.

Cell Cultures and Drug Treatments. Solutions of synthetic imidazole-4,5-dicarboxamide (I45DC) derivatives, purvalanol A, olomoucine (both purchased from Sigma, St. Louis, MO), and flavopiridol (a generous gift from Dr. Gunda Georg, University of Kansas, Lawrence, KS) were dissolved and serially diluted in dimethyl sulfoxide (DMSO). Suspended cultures of human HL-60 promyelocytic leukemia cells (from American Type Culture Collection, Manassas, VA) were maintained in continuous exponential growth by twice-a-week passage in RPMI 1640 medium supplemented with 8.25% fetal bovine calf serum (FCS; Atlanta Biologicals, Norcross, GA) and penicillin (100 IU/mL)–streptomycin (100 μ g/mL) and incubated in the presence or absence (control) of drugs at 37 °C in a humidified atmosphere containing 5% CO_2 . Since drugs were supplemented to the culture medium in 1- μ L aliquots, the concentration of vehicle (0.2% DMSO) in the final incubation volume (0.5 mL) was shown to not affect the growth and metabolic activity of control HL-60 cells incubated in the absence of drugs.³⁶

Cell Proliferation Assay. HL-60 cells suspended in FCS-containing RPMI 1640 medium were grown at 37 °C in 48-well Costar cell culture plates for up to 4 days in the presence or absence (control) of I45DCs in order to evaluate their antiproliferative activity. Decreasing concentrations of cells, such as 12.5×10^4 and 3.75×10^4 cells/0.5 mL/well, were initially plated in triplicate at time 0 in order to collect control samples with approximately equal cell densities after 2 and 4 days in culture, respectively. The proliferation of drug-treated cells was assessed from their mitochondrial ability to bioreduce the 3-(4,5-dimethylthiazol-2-yl)-5-(3-carboxymethoxyphenyl)-2-(4-sulfophenyl)-2H-tetrazolium (MTS) reagent (Promega, Madison, WI) in the presence of phenazine methosulfate (PMS; Sigma, St. Louis, MO) into a water-soluble formazan product that absorbs at 490 nm.⁴⁶ After 2 or 4 days in culture, control and drug-treated cell samples (about $10^6/0.5$ mL/well for controls) were further incubated at 37 °C for 3 h in the dark in the presence of 0.1 mL of MTS:PMS (2:0.1) reagent and their relative metabolic activity was estimated by recording the absorbance at 490 nm, using a Cambridge model 750 automatic microplate reader (Packard, Downers Grove, IL). Blank values for culture medium supplemented with MTS:PMS reagent in the absence of cells were subtracted from the results.³⁶

DNA Synthesis. To estimate the rate of DNA synthesis, HL-60 cells were resuspended in fresh FCS-containing RPMI 1640 medium at a density of 7.5×10^5 cells/0.5 mL, incubated at 37 °C for 2 h in the presence or absence (control) of drugs and then pulse-labeled for an additional 30 min with 1 μ Ci of [methyl- 3H]thymidine (50 Ci/mmol; Amersham, Arlington Heights, IL). The incubations were terminated by the addition of 0.5 mL of 10% trichloroacetic acid (TCA). After holding on ice for 15 min, the acid-insoluble material was recovered over Whatman GF/A glass microfiber filters and washed thrice with 2 mL of 5% TCA and twice with 2 mL of 100% EtOH. After drying the filters, the radioactivity bound to the acid-precipitable material was determined by liquid scintillation counting in 6 mL of Bio-Safe NA (Research Products International, Mount Prospect, IL).³⁶ Data of all biochemical experiments were analyzed using Student's *t*-test with the level of significance set at $P < 0.05$.

Molecular Modeling: Spartan Calculations. The two conformers of **22** were built independently in silico with an intramolecular hydrogen bond in each and minimized with the PM3 force field to their equilibrium geometries. This experiment was repeated a total of 10 times for each conformation, where the starting point for minimization was slightly varied each time as a result of the building process. The conformer with the aniline as the intramolecular hydrogen bond donor was -1.07 ± 0.04 kcal mol $^{-1}$ lower in energy, by this analysis, than the conformer with the aniline as the hydrogen bond acceptor. The amino acid torsion angles for each conformer in all runs approximated the extended conformation.

Acknowledgment. This study was supported in part by grants from the National Institutes of Health (National Cancer Institute 1R01 CA86842-05 and Center of Biomedical Research Excellence 1P20 RR15563-04 with matching funds from the State of Kansas), the Howard Hughes Medical Institute (Biological Sciences Education Grant), Kansas State University (Terry C. Johnson Center for Basic Cancer Research), Bowdoin College (Faculty Research Fund), and the National Science Foundation (NSF-MRI #0116416). We thank Elizabeth A. Stemmler (Bowdoin College) for mass spectrometry assistance and Gunda Georg (University of Kansas) for providing us with flavopiridol.

Supporting Information Available: NMR spectra, HPLC traces, theorized binding modes. This material is available free of charge via the Internet at <http://pubs.acs.org>.³⁷

References

- Hanahan, D.; Weinberg, R. A. The hallmarks of cancer. *Cell* **2000**, *100*, 57–70.
- Dash, B. C.; El-Deiry, W. S. Cell cycle checkpoint control mechanisms that can be disrupted in cancer. *Methods Mol. Biol.* **2004**, *280*, 99–161.
- Kastan, M. B.; Bartek, J. Cell-cycle checkpoints and cancer. *Nature* **2004**, *432*, 316–323.
- Sherr, C. J.; Roberts, J. M. Living with or without cyclins and cyclin-dependent kinases. *Genes Dev.* **2004**, *18*, 2699–2711.
- Mazumder, S.; DuPree, E. L.; Almasan, A. A dual role of cyclin E in cell proliferation and apoptosis may provide a target for cancer therapy. *Curr. Cancer Drug Targets* **2004**, *4*, 65–75.
- Lee, M. H.; Yang, H. Y. Regulators of G1 cyclin-dependent kinases and cancers. *Cancer Metastasis Rev.* **2003**, *22*, 435–449.
- Hanks, S. K. Genomic analysis of the eukaryotic protein kinase superfamily: a perspective. *Genome Biol.* **2003**, *4*, 111.
- Manning, G.; Whyte, D. B.; Martinez, R.; Hunter, T.; Sudarsanam, S. The protein kinase complement of the human genome. *Science* **2002**, *298*, 1912–1934.
- Dancey, J.; Sausville, E. A. Issues and progress with protein kinase inhibitors for cancer treatment. *Nat. Rev. Drug Discovery* **2003**, *2*, 296–313.
- Levitzi, A. Protein kinase inhibitors as a therapeutic modality. *Acc. Chem. Res.* **2003**, *36*, 462–469.
- Noble, M. E.; Endicott, J. A.; Johnson, L. N. Protein kinase inhibitors: insights into drug design from structure. *Science* **2004**, *303*, 1800–1805.

- (12) Pearson, M. A.; Fabbro, D. Targeting protein kinases in cancer therapy: a success? *Expert Rev. Anticancer Ther.* **2004**, *4*, 1113–1124.
- (13) Sawyer, T. K. Novel oncogenic protein kinase inhibitors for cancer therapy. *Curr. Med. Chem., Anticancer Agents* **2004**, *4*, 449–455.
- (14) Sausville, E. A. Cyclin-dependent kinase modulators studied at the NCI: pre-clinical and clinical studies. *Curr. Med. Chem. Anti-Cancer Agents* **2003**, *3*, 47–56.
- (15) Gladden, A. B.; Diehl, J. A. Cell cycle progression without cyclin E/CDK2: breaking down the walls of dogma. *Cancer Cell* **2003**, *4*, 160–162.
- (16) Aleem, E.; Berthet, C.; Kaldis, P. Cdk2 as a master of S phase entry: fact or fake? *Cell Cycle* **2004**, *3*, 35–37.
- (17) Hinds, P. W. Cdk2 dethroned as master of S phase entry. *Cancer Cell* **2003**, *3*, 233–245.
- (18) Shapiro, G. I. Preclinical and clinical development of the cyclin-dependent kinase inhibitor flavopiridol. *Clin. Cancer Res.* **2004**, *10*, 4270S–4275S.
- (19) Newcomb EW. Flavopiridol: pleiotropic biological effects enhance its anti-cancer activity. *Anticancer Drugs* **2004**, *15*, 411–419.
- (20) García-Echeverría, C.; Traxler, P.; Evans, D. B. ATP site-directed competitive and irreversible inhibitors of protein kinases. *Med. Res. Rev.* **2000**, *20*, 28–57.
- (21) Haesslein, J.-L.; Jullian, N. Recent advances in cyclin-dependent kinase inhibition. Purine-based derivatives as anti-cancer agents. Roles and perspectives for the future. *Curr. Top. Med. Chem.* **2002**, *2*, 1037–1050.
- (22) Cherry, M.; Williams, D. H. Recent kinase and kinase inhibitor X-ray structures: mechanisms of inhibition and selectivity insights. *Curr. Med. Chem.* **2004**, *11*, 663–673.
- (23) Honma, T.; Hayashi, K.; Aoyama, T.; Hashimoto, N.; Machida, T.; Fukasawa, K.; Iwama, T.; Ikeura, C.; Ikuta, M.; Suzuki-Takahashi, I.; Iwasawa, Y.; Hayama, T.; Nishimura, S.; Morishima, H. Structure-based generation of a new class of potent cdk4 inhibitors: New *de novo* design strategy and library design. *J. Med. Chem.* **2001**, *44*, 4615–4627.
- (24) Goldberg, D. R.; Butz, T.; Cardozo, M. G.; Eckner, R. J.; Hammach, A.; Huang, J.; Jakes, S.; Kapadia, S.; Kashem, M.; Lukas, S.; Morwick, T. M.; Panzenbeck, M.; Patel, U.; Pav, S.; Peet, G. W.; Peterson, J. D.; Prokopowicz, A. S., III; Snow, R. J.; Sellati, R.; Takahashi, H.; Tan, J.; Tschantz, M. A.; Wang, X.-J.; Wang, Y.; Wolak, J.; Xiong, J.; Moss, N. Optimization of 2-phenylaminoimidazo[4,5-h]isoquinolin-9-ones: Orally active inhibitors of lck kinase. *J. Med. Chem.* **2003**, *46*, 1337–1349.
- (25) De Bondt, H. L.; Rosenblatt, J.; Jancarik, J.; Jones, H. D.; Morgan, D. O.; Kim, S. H. Crystal structure of cyclin-dependent kinase 2. *Nature* **1993**, *363*, 595–602.
- (26) Schulze-Gahmen, U.; Brandsen, J.; Jones, H. D.; Morgan, D. O.; Meijer, L.; Vesely, J.; Kim, S. H. Multiple modes of ligand recognition: crystal structures of cyclin-dependent protein kinase 2 in complex with ATP and two inhibitors, olomoucine and isopentenyladenine. *Proteins* **1995**, *22*, 378–391.
- (27) Gray, N. S.; Wodicka, L.; Thunnissen, A. M.; Norman, T. C.; Kwon, S.; Espinoza, F. H.; Morgan, D. O.; Barnes, G.; LeClerc, S.; Meijer, L.; Kim, S. H.; Lockhart, D. J.; Schultz, P. G. Exploiting chemical libraries, structure, and genomics in the search for kinase inhibitors. *Science* **1998**, *281*, 533–538.
- (28) De Azevedo, W. F., Jr.; Mueller-Dieckmann, H. J.; Schulze-Gahmen, U.; Worland, P. J.; Sausville, E.; Kim, S. H. Structural basis for specificity and potency of a flavonoid inhibitor of human CDK2, a cell cycle kinase. *Proc. Natl. Acad. Sci., U.S.A.* **1996**, *93*, 2735–2740.
- (29) Kim, Kyoung, M.; Cho, Y.-H.; Kim, J. M.; Chun, M. W.; Lee, S. K.; Lim, Y.; Lee, C.-H. Inhibition of cell-cycle progression in human promyelocytic leukemia HL-60 cells by MCS-C2, novel cyclin-dependent kinase inhibitor. *J. Microbiol. Biotechnol.* **2003**, *13*, 607–612.
- (30) Baures, P. W.; Rush, J. R.; Wiznycia, A. V.; Desper, J.; Helfrich, B. A.; Beatty, A. M. Intramolecular hydrogen bonding and intermolecular dimerization in the crystal structures of imidazole-4,5-dicarboxylic acid derivatives. *Cryst. Growth Des.* **2002**, *2*, 653–664.
- (31) Li, L.; Shakhnovich, E. I.; Mirny, L. A. Amino acids determining enzyme–substrate specificity in prokaryotic and eukaryotic protein kinases. *Proc. Natl. Acad. Sci., U.S.A.* **2003**, *100*, 4463–4468.
- (32) Naumann, T.; Matter, H. Structural classification of protein kinases using 3D molecular interaction field analysis of their ligand binding sites: Target family landscapes. *J. Med. Chem.* **2002**, *45*, 2366–2378.
- (33) Wiznycia, A. V.; Baures, P. W. An improved method for the synthesis of dissymmetric *N,N'*-disubstituted imidazole-4,5-dicarboxamides. *J. Org. Chem.* **2002**, *67*, 7151–7154.
- (34) Wiznycia, A. V.; Rush, J. R.; Baures, P. W. Synthesis of symmetric bis-imidazole-4,5-dicarboxamides bearing amino acids. *J. Org. Chem.* **2004**, *69*, 8489–8491.
- (35) Cory, A. H.; Owen, J. C.; Barltrop, J. A.; Cory, J. G. Use of an aqueous soluble tetrazolium/formazan assay for cell growth assays in culture. *Cancer Commun.* **1991**, *3*, 207–212.
- (36) Wu, M.; Wang, B.; Perchellet, E. M.; Sperflage, B. J.; Stephany, H. A.; Hua, D. H.; Perchellet, J. P. Synthetic 1,4-anthracenediones, which block nucleoside transport and induce DNA fragmentation, retain their cytotoxicity in daunorubicin-resistant HL-60 cell lines. *Anti-cancer Drugs* **2001**, *12*, 807–819.
- (37) Villerbu, N.; Gaben, A. M.; Redeuilh, G.; Mester, J. Cellular effects of purvalanol A: A specific inhibitor of cyclin-dependent kinase activities. *Int. J. Cancer* **2002**, *97*, 761–769.
- (38) Chang, Y. T.; Gray, N. S.; Rosania, G. R.; Sutherland, D. P.; Kwon, S.; Norman, T. C.; Sarohia, R.; Leost, M.; Meijer, L.; Schultz, P. G. Synthesis and application of functionally diverse 2,6,9-trisubstituted purine libraries as CDK inhibitors. *Chem. Biol.* **1999**, *6*, 361–375.
- (39) Harmse, L.; van Zyl, R.; Gray, N.; Schultz, P.; Leclerc, S.; Meijer, L.; Doerig, C.; Havlik, I. Structure–activity relationships and inhibitory effects of various purine derivatives on the *in vitro* growth of *Plasmodium falciparum*. *Biochem. Pharmacol.* **2001**, *62*, 341–348.
- (40) Spartan '02, Wave function Inc., 18401 Von Karman Avenue, Suite 370, Irvine, CA 92612.
- (41) Rush, J. R.; Sandstrom, S. L.; Yang, J.; Davis, R.; Prakash, O.; Baures, P. W. Intramolecular hydrogen bond strength and pK_a determination of *N,N'*-disubstituted imidazole-4,5-dicarboxamides. *Org. Lett.* **2005**, *7*, 135–138.
- (42) Pierce, A. C.; Haar, E.-t.; Binch, H. M.; Kay, D. P.; Patel, S. R.; Li, P. CH \cdots O and CH \cdots N hydrogen bonds in ligand design: A novel quinazolin-4-ylthiazol-2-ylamine protein kinase inhibitor. *J. Med. Chem.* **2005**, *48*, 1278–1281.
- (43) Perez-Roger, I.; Ivorra, C.; Diez, A.; Cortes, M. J.; Poch, E.; Sanz-Gonzalez, S. M.; Andres, V. Inhibition of cellular proliferation by drug targeting of cyclin-dependent kinases. *Curr. Pharm. Biotechnol.* **2000**, *1*, 107–116.
- (44) Richard, C.; Matthews, D.; Duivenvoorden, W.; Yau, J.; Wright, P. S.; Th'ng, J. P. H. Flavopiridol sensitivity of cancer cells isolated from ascites and pleural fluids. *Clin. Cancer Res.* **2005**, *11*, 3523–3529.
- (45) Knockaert, M.; Lenormand, P.; Gray, N.; Schultz, P.; Pouyssegur, J.; Meijer, L. p42/p44 MAPKs are Intracellular Targets of the CDK Inhibitor Purvalanol. *Oncogene* **2002**, *21*, 6413–6424.
- (46) Cory, A. H.; Owen, J. C.; Barltrop, J. A.; Cory, J. G. Use of an aqueous soluble tetrazolium/formazan assay for cell growth assays in culture. *Cancer Commun.* **1991**, *3*, 207–212.

JM050160R